On the evaluation of the antimicrobial effect of grape seed extracts and cold atmospheric plasma on the dynamics of *Listeria monocytogenes* in novel multiphase 3D viscoelastic models

Melina Kitsiou [a, b], Lisa Purk [a, b], Christina Ioannou [a], Thomas Wantock [c], Gavin Sandison [c], Thomas Harle [c], Jorge Gutierrez-Merino [d], Oleksiy V. Klymenko [a], and Eirini Velliou [a, b*]

[a] *School of Chemistry and Chemical Engineering, University of Surrey, Guildford, GU2 7XH, UK.*

[b] *Centre for 3D models of Health and Disease, Division of Surgery and Interventional Science, University College London, London, W1W 7TY, UK.*

[c] *Fourth State Medicine Ltd, Longfield, Fernhurst, Haslemere, GU27 3HA, UK*

[d] *School of Biosciences and Medicine, University of Surrey, Guildford, GU2 7XH, UK.*

*Corresponding author. E-mail address: *e.velliou@ucl.ac.uk*

Abstract

The demand for products that are minimally processed and produced in a sustainable way, without the use of chemical preservatives or antibiotics have increased over the last years. Novel non-thermal technologies such as cold atmospheric plasma (CAP) and natural antimicrobials such as grape seed extract (GSE) are attractive alternatives to conventional food decontamination methods as they can meet the above demands. The aim of this study was to investigate the microbial inactivation potential of GSE, CAP (in this case, a remote air plasma with an ozone-dominated RONS output) and their combination against *L. monocytogenes* on five different 3D *in vitro* models of varying rheological, structural, and biochemical composition. More specifically, we studied the microbial dynamics, as affected by 1% (w/v) GSE, CAP or their combination, in three monophasic Xanthan Gum (XG) based 3D models of relatively low viscosity (1.5%, 2.5% and 5% w/v XG) and in a biphasic XG/Whey Protein (WPI) and a triphasic XG/WPI/fat model. A significant microbial inactivation (comparable to liquid broth) was achieved in presence of GSE on the surface of all monophasic models regardless of their viscosity. In contrast, the GSE antimicrobial effect was diminished in the multiphasic systems, resulting to only a slight disturbance of the microbial growth. In contrast, CAP showed better antimicrobial potential on the surface of the complex multiphasic models as compared to the monophasic models. When combined, in a hurdle approach, GSE/CAP showed promising microbial inactivation potential in all our 3D models, but less microbial inactivation in the structurally and biochemically complex multiphasic models, with respect to the monophasic models. The level of inactivation also depended on the duration of the exposure to GSE. Our results contribute towards understanding the antimicrobial efficacy of GSE, CAP and their combination as affected by robustly controlled changes of rheological and structural properties and of the biochemical composition of the environment in which bacteria grow. Therefore, our results contribute to the development of sustainable food safety strategies.

Keywords: natural antimicrobials, cold atmospheric plasma (CAP), 3D (food) model systems, microbial inactivation, *Listeria monocytogenes*, hurdle approach, food safety.

1. Introduction

Nowadays, the demand for minimally and environmentally friendly processed food products is rising (Dávila-Aviña et al., 2015; Pereira & Vicente, 2010). Therefore, researchers and the food industry have been focusing on replacing chemical preservatives and/or antibiotics with natural antimicrobials. In that context, fruit and vegetable by-products can be a valuable source of natural antimicrobials with the added benefit of valorising food waste (Chandrasekaran, 2012; Costello et al., 2018, 2019, 2021a, 2021b; Sabater et al., 2020; Sharma et al., 2021). At the same time, non-thermal technologies (NTTs) such as cold atmospheric plasma (CAP), ultrasound, pulsed electric fields and high-pressure processing have gained a lot of attention over the last years, as they can be considered more sustainable and less disruptive of the food product quality as compared traditional thermal processing technologies i.e., sterilization, pasteurisation (Bahrami et al., 2020; Costello et al., 2021a, 2021b; El Kadri et al., 2021; Mandal et al., 2018; Pankaj et al., 2018; Pereira & Vicente, 2010; Sunil et al., 2018; Tewari & Juneja, 2007).

Grape seed extract (GSE) is a grape by-product generated from the wine and juice industry, which is obtained from the seeds of the grapes (Chedea & Pop, 2019; Costa et al., 2022; Karnopp et al., 2017; Shrikhande, 2000). GSE is rich in polyphenols, and it can be an effective antioxidant and antimicrobial agent. The antimicrobial activity of GSE has been linked to multiple mechanisms of action, including the polyphenols' ability (i) to penetrate the bacterial cell wall, (ii) to inactivate extracellular enzymes and (iii) to form complexes with metal ions

depleting the bacterial environment of those ions (Begg, 2019; Corrales et al., 2009; Silván et al., 2013). The most frequent methods used to determine the antimicrobial effect of grape by-products are the agar/disk diffusion test and the minimum inhibitory concentration (Baydar et al., 2004; Delgado Adámez et al., 2012; Katalinić et al., 2010; Oliveira et al., 2013; Silva et al., 2018; Xu et al., 2016). With these methods, grape by-products have demonstrated substantial antibacterial activity against Gram-positive bacteria such as *Listeria monocytogenes, Bacillus cereus, Enterococcus faecalis, Enterococcus faecium, Staphylococcus aureus, Staphylococcus epidermidis and Mycobacterium smegmatis* (Baydar et al., 2006; Corrales et al., 2009; Silva et al., 2018). However, studies regarding the antimicrobial activity against Gram-negative bacteria are contradictory. For example, Corrales et al., (2009) have shown that 1% (w/v) GSE did not inhibit *E. coli* and *S.* Typhimurium based on an agar diffusion test (Corrales et al., 2009). On the contrary, in a study by Baydar et al., (2006) using the same methodology, inhibition was observed for those bacteria (Baydar et al., 2006). The above methods are valuable for the preliminary evaluation of the antimicrobial activity of a substance. However, no information is provided regarding the precise quantitative inactivation dynamics of the microorganism under study. Therefore, the robust design of an industrial or clinical treatment procedures cannot be based solely on those data. To the author's best knowledge, limited number of studies exist on the quantification of the antimicrobial efficacy of GSE (microbial dynamics). Most of those studies have tested the antimicrobial activity of GSE in nutrient broths or/and certain food products, primarily meat and fish products, making the results very specific to the actual food product (Ahn et al., 2004, 2007; Sagdic et al., 2011; Sivarooban et al., 2007; Zhao et al., 2020). For example, Sivarooban et al. (2007) observed a reduction of 2 log CFU/ml in the concentration of *L. monocytogenes* after 24h of exposure to 1% (w/v) GSE in liquid nutrient medium (TSBYE). The initial inoculum population was approx. $5x10^6$ CFU/ml (Sivarooban et al., 2007). We recently investigated the microbial dynamics of *L.*

monocytogenes, *E. coli* and *S.* Typhimurium in the presence of GSE in liquid nutrient medium (TSBYE). We observed that GSE had great inactivation efficacy against *L. monocytogenes* at 1% (w/v) GSE concentration. The level of inactivation after 24 hours was affected by the initial microbial inoculum level, the GSE concentration and the growth phase of the cells, i.e., stationary phase was more resistant to GSE as compared to exponential phase cells. *E. coli* and *S.* Typhimurium were more tolerant to GSE in comparison to *L. monocytogenes* (Kitsiou et al., 2023). Previous studies on the antimicrobial activity of GSE in real food products have reported good antimicrobial efficacy of GSE when treating fresh produce such as tomato surfaces. However, when GSE were utilized in more complex food products with higher structural complexity as well as higher protein and fat content such as ground beef and turkey frankfurters, the antibacterial activity was diminished (Ahn et al., 2007; Bisha et al., 2010; Sivarooban et al., 2007).

Indeed, the biochemical composition and the physicochemical and structural characteristics of a food system can influence the microbiological response to any hurdle/process/treatment (Costello et al., 2019, 2021a; El Kadri et al., 2021; Garcia-Gonzalez et al., 2009; Smet et al., 2017; Vandekinderen et al., 2009; Verheyen et al., 2019, 2020). Therefore, results on antimicrobial efficacy from screening tests in simple controlled laboratory nutrient media such as Tryptic Soy or Brain Heart Infusion broths are not fully representative, as the planktonic nature of microbial broth and the lack of concentration gradients of the stress factor (e.g., natural antimicrobial concentration) can lead to a completely different microbial response as compared to a solid or a solid(like) environment. In the latter, bacteria are immobilised and form colonies, aggregates or biofilms which can respond very differently to a stress factor or a treatment approach, due to (i) gradients that can occur within the sold matrix (ii) accumulation of metabolic by-products such as acid for example which can lead to an increased bacterial resistance to the treatment via cross-protection mechanisms (Baka et al., 2017; Costello et al.,

2018, 2019, 2021a, 2021b ; Skandamis & Jeanson, 2015; Smet et al., 2017; Velliou et al., 2013; Wang et al., 2017). For this reason, the scientific community has been focusing lately on performing microbial studies in 3D *in vitro* models, using a variety of gelling agents and compositions i.e., gelatin, dextran, xanthan gum, agar as well as their combinations (Aspridou et al., 2014; Costello et al., 2018, 2019, 2021a; Das et al., 2015; Mertens et al., 2009; Skandamis et al., 2000; Velliou et al., 2013; Wang et al., 2017). For example, Smet et al. (2018) demonstrated higher CAP inactivation of cells grown planktonically as compared to cells grown on structured 3D models i.e., gelatin at 5% (w/v). Additionally, Costello et al. (2021a) observed that cells inactivated in a liquid carrier, regardless of whether they were (pre-) grown planktonically or as surface colonies, were more tolerant to the CAP treatment compared to those that were inactivated on a 3D *in vitro* model with 1.5% (w/v) XG. This indicates that liquid systems/carriers provide a protective effect against CAP treatment. Additionally, Costello et al., (2018) showed that the antimicrobial effect of nisin (140 IU/ml) against *L. innocua* was reduced when incorporated in 3D models (3-7% w/v Xanthan Gum) for submerged growth but increased for surface growth when combined with a suboptimal incubation temperature (10 °C). Similar findings showing substantial differences in microbial growth and/or inactivation in solids as compared to liquid systems have been reported in other studies (Antwi et al., 2008; Aryani et al., 2016; Baka et al., 2016; El Kadri et al., 2021; Karina et al., 2011; Piyasena et al., 2003; Pol et al., 2001; Wang et al., 2017). Overall, using 3D *in vitro* models, enables better reproducibility and better control of biochemical, biomechanical and structural components, as compared to actual food products (that vary even from batch-to-batch and have properties very specific to the product). Furthermore, those models allow a more realistic spatial organisation and growth of microorganisms as compared to simple *in vitro* systems (liquid broths). Consequently, 3D models enable the conduction of mechanistic studies of microbial responses to treatment approaches.

The aim of this work is to investigate, for the first time, the impact of structural and biochemical complexity of 3D *in vitro* models, i.e., monophasic Xanthan Gum-based 3D models of various gelling agent concentrations as well as multiphasic Xanthan Gum-based 3D models containing additional protein and fat phases, on the microbial response of *L. monocytogenes*., i.e., foodborne pathogen that causes major public health concern, to (i) GSE (ii) CAP and (iii) GSE in combination with CAP. As described above, CAP is a NTT which has generally shown good microbial inactivation potential in broths, some 3D models and some foods (Costello al., 2021a; El Kadri et al., 2021; Mandal et al., 2018; Patange et al., 2019; Smet et al., 2018; Thirumdas et al., 2014). Such a hurdle approach is promising, considering that both GSE and CAP treatments are mild processes which might have a higher microbial inactivation potential when acted in combination, in contrast to individual treatments that, generally, have lower inactivation potential (especially in comparison to classic approaches such as heat treatment) (Costello et al., 2021a; Cui et al., 2016a, 2016c; Khan et al., 2017; Leistner, 2000; Matan et al., 2014, 2015; Millan-Sango et al., 2015; Mosqueda-Melgar et al., 2008; Peleg, 2020). Our work sheds light on the understanding of the impact of structural complexity on the response of *L. monocytogenes* to GSE as well as GSE combined with CAP, therefore, contributing to the design of alternative, sustainable microbial inactivation strategies.

2. Materials and methods

2.1. Inoculum preparation

Stock cultures of *L. monocytogenes* 10403S were stored in Tryptone Soy Broth (TSB, Oxoid Ltd, UK) supplemented with 15% glycerol at -80 °C. The inoculum preparation took place as previously described (Costello et al., 2018, 2019, 2021a, 2021b; Kitsiou et al., 2023; Velliou et al., 2010, 2011a, 2011b, 2012, 2013). More specifically, a loopful of thawed culture was inoculated in 20 ml TSB supplemented with 0.6% w/v of Yeast Extract (Oxoid Ltd, UK)

(TSBYE) and cultured for 9.5 h in a shaking incubator at 37 °C and 175 rpm. Thereafter, 20 µl were transferred in 20 ml TSBYE and cultured for another 15 h until early stationary phase was reached (approximately 10^9 CFU/ml).

2.2. Grape seed extracts (GSE)

The present study used commercially available grape seed extract (GSE) (Bulk, UK). The GSE powder contained a minimum of 95% oligomeric proanthocyanidin. We, therefore, consider the powder almost pure on oligomeric proanthocyanidins. The GSE powder was dissolved in TSBYE at concentration 1% w/v for both the liquid (broth) and 3D model experiments. This GSE concentration was determined based on our previous study in TSBYE broth, which showed that GSE (1% w/v) substantially inactivated (~3 log CFU/ml after 24 h) *L. monocytogenes* in liquid nutrient medium (TSBYE) (Kitsiou et al., 2023). Additionally, other studies previously demonstrated that 1% w/v GSE significantly inactivated *L. monocytogenes*, as determined by agar diffusion tests (Ahn et al., 2007; Baydar et al., 2006; Corrales et al., 2009).

2.3 Preparation of viscoelastic food model systems

The preparation of the monophasic and biphasic 3D models followed a similar procedure to our previously published work (Costello et al., 2018, 2021a; El Kadri et al., 2021; Velliou et al., 2013).

More specifically, *for the monophasic system*, Xanthan Gum (XG) (Xantural® 75; CP Kelco, UK) at concentrations 1.5%, 2.5% and/or 5% (w/v) was added to TSBYE. These concentrations of XG were selected to cover a wide range of viscosities, as we have previously studied (Costello et al., 2018, 2021a; Mertens et al., 2009; Velliou et al., 2013). Thereafter, the

mixtures were mechanically stirred (2,000 rpm) for at least 5 min until complete homogeneity was achieved (Omni Mixer Homogenizer, Omni International Inc., USA). The homogenized mixture was then added in 15 ml falcon tubes (approx. 9 g of the mixture per falcon tube) and centrifuged at 4000 ×g for at least 30 min to eliminate the entrapped air bubbles. Thereafter, the 3D models were autoclaved at 121°C for 30 min. To remove the remaining air bubbles, the autoclaved 3D models were centrifuged again at 4000 ×g for 15 min.

For *the biphasic system*, 10% (w/v) Whey Protein Isolate (WPI) (Bacarel, UK), 5% (w/v) XG and NaCl (1% w/v) (Fisher Scientific, UK) were added in TSBYE and magnetically stirred (Bibby Sterilin Ltd, UK). The addition of NaCl ensured phase separation by increasing the ionic strength of the system (Polyakov et al., 1997). This low concentration of NaCl is insufficient to induce osmotic stress in the cells (Noriega et al., 2014). Thereafter, the same procedure as the monophasic 3D models was followed i.e., the biphasic system was mechanically stirred, centrifuged, autoclaved, and centrifuged again. (Costello et al., 2018, 2021a; El Kadri et al., 2021; Velliou et al., 2013)

For *the triphasic system*, the previous biphasic system was enriched with 10% (v/v) of commercially available sunflower oil (made in the UK using sunflower seeds from EU/non-EU countries for Co-operative Group Ltd). More specifically, the fat phase was added to the homogenous solution of WPI, NaCl and TSBYE and mechanically stirred (2 min at 2,000 rpm) before the addition of XG. Afterwards, the procedure was carried on as previously described for the biphasic system. Images of the developed 3D models can be seen in Figure A2 in the Appendix.

For the evaluation of the effect of natural antimicrobials, GSE was added to TSBYE along with the other model components to a final concentration in the models of 1% (w/v) (see also section 2.2).

To prepare the models for the microbial dynamic studies, the following procedure was followed: For the *monophasic systems*, the models were placed into a 24-well plate, i.e., surface area of approx. 2 cm^2), to ensure reproducibility of their size. This took place via pipetting, using pipettes for viscous media (MICROMAN® E, Gilson Ltd., USA). For the *biphasic and triphasic systems*, due to their structure, pipetting was not possible and, therefore, the models were initially shaped using 3D printed moulds of the same size and surface area as the monophasic XG-based models. Thereafter, they were moved with a sterile tweezer into a 50 mm petri dish for the conduction of the microbial kinetic experiments and in 12 well-plates for any experimentation involving CAP treatment.

2.4. Rheological Characterization

For the rheological characterization of the 3D models the storage modulus G' (Pa) and the loss modulus G'' (Pa) were determined. Examination was carried out at 37 °C (as microbial growth took place at that temperature in the 3D models, which is the optimal temperature for growth of *L. monocytogenes*) conducting dynamic oscillatory measurements, as previously described by Costello et al. (2018).

The storage modulus G′ (Pa) and the loss modulus G′′ (Pa) were measured as functions of angular frequency ω from 0.1 to 100 (rad/s) using a rotational Physica MCR 200 rheometer (Physica MCR 200, Anton Paar GmbH, Germany) with a maximum strain of 2% and a Paar Physica circulating water bath to control the temperature (Viscotherm VT2, Anton Paar GmbH, Germany). For each viscoelastic system, a minimum of two independent replicates of at least two samples were analysed using a cone and plate geometry (50mm diameter, 2° angle). G′ and G′′ represent the elasticity and viscosity of the model, respectively. At least three

independent experiments were performed per condition/model to ensure statistical significance.

2.5. Scanning electron microscopy

Scanning electron microscopy analysis of the monophasic 5% (w/v) XG model has been previously described and published by our group (Costello et al., 2019). For the complex biphasic and triphasic 3D model systems microscopic analysis was carried out via SEM, (as previously described (Costello et al., (2019). More specifically, the samples (3D models) were fixed with 3% (v/v) formaldehyde solution for 1 h and then serially dehydrated in 20%, 40%, 60%, 80% and 100% ethanol (99.6%) and washed twice with Dulbecco's Phosphate Buffered Saline (DPBS). Thereafter, the dehydrated, fixed samples were mounted on a 13 mm 14 aluminium stub (Agar Scientific) and sputter coated with gold twice to a 272 thickness of 6 nm using an Emitech K550X Sputter Coater (Quorum Technologies, Ashford, UK) with a target current of 20 mA for 1 min. Then, the samples were observed under a JEOL JSM-7100F SEM microscope operated at 5 kV.

2.6. Microbial dynamics in the presence of GSE

To examine the antimicrobial activity of 1% (w/v) GSE added in TSBYE, monophasic, biphasic and triphasic systems (as described in section 2.3), early stationary phase cells of *L. monocytogenes* (grown as described in section 2.1), were appropriately diluted and inoculated (by pipetting) in either TSBYE (3 ml) or on the surface of the various 3D models as we have previously described (Costello et al., 2018, 2019). The initial cell concentration was approximately 10^5 CFU/ml for all systems under study. This initial inoculum concentration was selected as the most appropriate as it enables the observation of the microbial dynamics

i.e., inhibition or growth in the presence of the GSE. Additionally, *L. monocytogenes* was added in liquid and on the surface of the 3D models not containing GSE (controls).

After inoculation, the samples were incubated at 37 °C, i.e., optimal growth temperature for *Listeria*. The bacterial survival was systematically monitored for up to 24 h post-treatment (at 0, 2, 4, 8, 12, 18, 24 h). Thereafter, all samples were analysed, i.e., determination of colony formation units, as previously described (Costello et al., 2018, 2019). Briefly, the samples were added in phosphate buffered saline (PBS, Oxoid Ltd., UK) at a 1/10 dilution. The monophasic XG-based models were homogenised using a vortex mixer (Onilab LLC., USA) and the multiphasic systems using a stomacher for at least 1 minute (Colworth Stomacher 80, Seward, UK). The surviving population was enumerated using the spread plate count method in non-selective agar i.e., Tryptone Soy Agar supplemented with 0.6% of Yeast Extract (TSAYE, Oxoid Ltd, UK).

2.7. CAP experimental set-up

The CAP device used (Figure 1) in this study has been developed and provided by Fourth State Medicine Ltd. We have previously characterised the configuration of the device (El Kadri et al., 2021). Briefly, the generator of CAP in this apparatus is a dielectric barrier discharge in a remote and enclosed configuration, whereby the plasma source is contained in an electrically-shielded enclosure and separated from the treatment target by a tube, with no direct line of sight. The gas used for ionization is compressed air (25 °C, 3 bars), and its flow rate (0-5 L/min) is controlled by a needle valve and a flow meter mounted on the enclosure. The chemical composition of the plasma output varies based on the input air flow rate (Please see table A1 of appendix). For example, at flow rate 1 L/min more reactive nitrogen species (RNS– primarily NO_x compounds, NO_2 and NO) are produced in comparison with 5 L/min at which

the air flow is enriched with more reactive oxygen species (ROS– primarily O_3). To that end, measurements were obtained using a calibrated Sauermann E4500 flue gas analyser and a calibrated 2B technologies Model 106-MH ozone monitor. The data were collected by Fourth State Medicine Ltd. by connecting the generator output to each piece of equipment and measurements were taken at different flow rates. The NO_2 sensor exhibits cross-sensitivity to O_3. Therefore, to ensure accurate measurements, O_3 was first monitored until the sensor reading was below 10ppb, followed by the measurement of NO_2 and NO contents. Additionally, measurements provided by Fourth State Medicine Ltd using a similar device running on compressed air, showed the presence of other nitrogen-containing, NO_z, compounds, including a mixture of N_2O, HONO, and other compounds, alongside O_3. The total concentration of these NO_z species was approximately 100-200 ppm and decreased with increasing flow rates (Fourth State Medicine Ltd, 2023). The concentration of ROS followed an opposite trend i.e., increased with increasing flow rates reaching approximately 960 ppm at flow rate 5 L/min.

In terms of the structure of the device, the plasma effluent (air flow containing RONS) passes through a 1m plastic tube (Tygon®, 6.4 mm outer diameter, 1.6 mm wall thickness, VWR, UK) which is connected to a nozzle. Nozzles of various sizes can be fitted to cover a well of a 12 and/or 24-well plate (2.2 and 1.55 cm diameter respectively) and therefore direct the gas to the sample. All CAP experiments were conducted under a fume hood to allow the produced gas to safely escape. The plasma device was turned on at least 30 min before the sample treatment to ensure consistency of RONS outputs throughout the experiment. For the CAP treatment experiments, as described in section 2.3, monophasic 3D models were placed in 24-well plated and biphasic and triphasic systems in 12-well plates. The samples were treated with 5 L/min flow rate for 2 minutes. It should be stated that no experiments in liquid were conducted, and the microbial response to CAP (or CAP combined with GSE as described in the following section) was compared only between different 3D model systems. This is because

preliminary experiments have shown that for efficient inactivation in a liquid carrier a different flow rate of 1 L/min is required, which is enriched in RNS as compared to the used flow rate which contains more ROS. Therefore, additionally to structural differences of the carrier the CAP treatment would involve different reactive species, making a sound comparison between liquid and 3D model inaccurate.

2.8. Combined treatment: CAP and GSE

For the combined treatment of GSE and CAP in the 3D model systems, *L. monocytogenes* was inoculated on the surface of systems under study (monophasic, biphasic and triphasic) as described in section 2.4. All 3D models contained 1% (w/v) GSE, and the initial microbial population was 10^5 CFU/ml as described in section 2.4. The 3D models were incubated for a total of either 2 h or 8 h at 37 °C prior to CAP treatment. These incubation times were selected following our initial kinetic experiments with GSE only (section 2.4), to ensure we induce mild and moderate microbial inactivation from the exposure to GSE (but not very high inactivation, so that the combined experiments with CAP are meaningful). Thereafter, the 3D models were treated with CAP for 2 min at a flow rate of 5 L/min as described in section 2.7. The post-treatment survival of the microbial population was determined with plating, as described in section 2.4.

2.9. Statistical analysis

At least two independent experiments with three replicate samples were conducted for all conditions under study. When comparing two mean values, a t-test was used to confirm statistical significance ($p < 0.05$) while for multiple comparisons, a two-way ANOVA followed by Tukey's HSD post hoc was used to confirm statistically significant ($p < 0.05$) differences between independent experimental groups. In the plots below, the mean value is presented with

error bars representing the standard deviation. In cases where the viable cell count was below the detection limit (<10 CFU/ml) the number was set to 1 log CFU/ml. All statistical analysis was performed using GraphPad Prim and Microsoft Excel.

3. Results and discussion

As previously mentioned, in order to study the impact of grape seed extract (GSE) on the microbial dynamics of *L. monocytogenes* in *in vitro* 3D models, GSE was incorporated in three monophasic 3D models, with varying xanthan gum (XG) concentration (1.5, 2.5 and 5% w/v) as well as in structurally complex biphasic systems, containing XG and Whey Protein (WPI) (5% w/v XG, 10% w/v WPI) and triphasic systems, containing XG, WPI and fat (5% w/v XG, 10% w/v WPI, 10% v/v fat). Additionally, all developed 3D models were used to investigate the effect of the combination of GSE and CAP against the growth of *L. monocytogenes.*

To the authors' best knowledge this is the first study systematically investigating the antimicrobial effect of GSE individually and/or in combination with a novel non-thermal technology such as CAP in such solid-like 3D models, of robustly controlled structural and biochemical composition.

3.1. The impact of GSE on the microbial dynamics of L. monocytogenes on the surface of 3D multiphase 3D models.

As can be seen in Figure 2, 1% (w/v) GSE caused significant microbial inactivation in both liquid broth (TSBYE) as well as in all three monophasic 3D models, regardless of their viscosity (the inactivation rate, k_{max}, is approximately 0.9/min). The level of inactivation of the treated liquid samples was equal to 1.5, 2.4, and 2.9 log CFU/ml, after 8, 12, and 24 h respectively. The microbial dynamics also showed that 1% (w/v) GSE inhibited *L.*

362 *monocytogenes* in liquid to a similar level as all the monophasic 3D models, i.e., ~3 log CFU/ml
363 after 24 h. More specifically, after 8, 12, and 24 h the average microbial inactivation of the
364 treated samples was equal to 1.4, 2.2, and 2.9 log CFU/ml, respectively. Additionally, the
365 difference between the treated samples and the control samples for the three monophasic XG-
366 based systems was on average 6.5 log CFU/ml after 24 h. These findings collectively show that
367 changes in the surface viscosity of the monophasic gels did not affect the antimicrobial action
368 of GSE against *L. monocytogenes*.

369 The microbial dynamics shown in Figure 2 (e, f), demonstrate that the antibacterial activity
370 of GSE was greatly reduced when incorporated in the biphasic and triphasic 3D models. More
371 specifically, there was no bacterial inactivation in presence of 1% (w/v) GSE and even growth
372 of *L. monocytogenes* was observed (the microbial growth rate, μ_{max}, is approximately 1.2/h).
373 However, a slight but statistically significant disturbance in the microbial growth can be seen
374 as compared to the untreated samples (Figure 2e, 2f). More specifically, for the biphasic 3D
375 model, the difference in the viable cell population between the control and the treated sample
376 (1% w/v GSE) ranged from 0.2 to 0.5 log CFU/ml depending on the time point. After 24 h the
377 difference was equal to 0.4 log CFU/ml (Figure 2e). For the triphasic 3D model, the highest
378 disturbance in the growth was observed after 12 h (0.4 log CFU/ml) but after 24 h there was
379 no significant difference ($p>0.05$) between the treated and untreated sample (Figure 2f).

380 To the author's best knowledge this is the first study investigating the microbial inactivation
381 of GSE in 3D *in vitro* models with controlled biochemical composition and changing viscosity
382 and structure. As mentioned in the Introduction section, most studies investigating the
383 antimicrobial activity of GSE to date, have used liquid nutrient media or they have been
384 conducted in specific food products. Studies in liquid nutrient media, including our recently
385 published study (Kitsiou et al., 2023), show a clear and substantial effect of GSE against *L.*
386 *monocytogenes*, with the level of microbial inactivation depending on factors such as the initial

387 microbial load, the GSE concentration and the microbial growth phase, i.e., exponential or
388 stationary growth (Ahn et al., 2004, 2007; Sagdic et al., 2011; Sivarooban et al., 2007; Zhao et
389 al., 2020, Kitsiou et al., 2023). However, when moving from simple liquid systems to food
390 products, the GSE antimicrobial effect hugely varies, depending on the food product. For
391 example, Bisha et al. (2010) observed good antimicrobial efficacy of GSE against *L.*
392 *monocytogenes* on (smooth) tomato surfaces. The tomatoes were dipped in GSE solution
393 (0.125% w/v) for 2 and 10 min and the microbial inactivation directly after each treatment was
394 2 and 4 log CFU/ml, respectively. However, when GSE was utilized on more complex food
395 products with higher structural complexity as well as higher protein and fat content such as
396 ground beef and turkey frankfurters, the antibacterial activity was diminished (Ahn et al., 2007;
397 Bisha et al., 2010; Sivarooban et al., 2007). For instance, Ahn et al., (2007) reported growth
398 (instead of inactivation) of *L. monocytogenes* in cooked beef which was treated with 1% GSE
399 and stored at 4 °C for 9 days. These results follow a similar trend to our 3D models, i.e., good
400 antibacterial effect against *L. monocytogenes* on simple solid systems and very limited
401 antibacterial effect on biochemically and structurally complex food systems. Further to food
402 products, GSE has been utilised as part of 3D films, for packaging materials with antibacterial
403 properties (Corrales et al., 2009; Deng & Zhao, 2011). GSE incorporated in films, showed
404 some antimicrobial efficacy for both Gram-positive and Gram-negative bacteria tested. For
405 example, Deng & Zhao (2011), developed three types of films adding grape pomace extracts
406 (25% w/v) with either low methoxyl pectin, sodium alginate, and/or a mixture of sodium
407 alginate carrageenan, and cellulose gum. The antimicrobial activity was tested against *E. coli*
408 and *L. innocua* at initial load of approximately 10^5 CFU/ml. All GSE films had similar
409 antimicrobial effect against the tested microorganisms. More specifically, GSE had a
410 bacteriostatic effect against *E. coli* throughout the 24 h. However less antimicrobial effect was
411 observed against *L. inoccua,* whose final cell concentration after 24 h was 1.7 to 3.0 log

412 CFU/ml lower than the control. Additionally, when Corrales et al., (2009) added 1% GSE in
413 pea starch films to control *Brochothrix thermosphacta* in pork loins, the results showed a
414 reduction of 1.3 log CFU/ml (in comparison with the control) after 4 days at 4 °C. However,
415 after an initial reduction (until 4 days), growth was reported similar to the untreated sample
416 (Corrales et al., 2009).

417 Overall, the changes in the antimicrobial inactivation potential of GSE that we observe in
418 our 3D models, i.e., varying from substantial microbial inactivation on the surface monophasic
419 system regardless of their viscosity to only a slight microbial growth disturbance on the surface
420 of biphasic and triphasic 3D models, can be attributed to several reasons. Factors that could
421 affect the antimicrobial activity could be linked to the rheological properties, the 3D
422 microstructure, the biochemical composition of the developed systems as well as the
423 environmental conditions (e.g., incubation temperature) or the combination of those factors.

424 Existing literature in the presence of natural antimicrobials in controlled 3D *in vitro* models
425 has emerged but is limited. For example, we have previously investigated the effect of
426 sublethal concentration of nisin (140 IU/ml) against *L. innocua* in liquid and monophasic XG
427 based 3D models, of varying XG concentration (3-7% w/v XG). The antimicrobial effect of
428 nisin was generally low both in liquid and in the 3D models, in contrast to the effect of GSE
429 that we observed in our current study (Figure 2). However, similarly to our current findings for
430 GSE, no differences in the response to nisin between liquid broth and the 3D monophasic XG
431 gum models was observed at 37 °C, regardless of the changes in viscosity. The synergistic
432 impact of structure (more rigid gel as compared to gels of lower XG gum concentration or
433 liquid both) with nisin was observed only at 10 °C which is a much lower temperature than the
434 optimal growth temperature for *Listeria* (37 °C) (Costello et al., 2018).

As shown on Table 1, when comparing the rheological properties of the monophasic (5% w/v XG) to the multiphasic systems, i.e., biphasic (5% w/v XG and WPI) and triphasic (5% w/v XG and WPI and fat), the latter have a higher viscosity (an increased firmness/rigidness of the gels). Generally, it has been reported that increasing the firmness can cause diffusion limitations of nutrients leading to a reduced microbial growth but, at the same time, it can cause diffusional limitations of antimicrobials, which can lead to reduced microbial inhibition (Aspridou et al., 2014; Costello et al., 2018, 2019; Makariti et al., 2021; Skandamis & Jeanson, 2015; Velliou et al., 2013). For example, Skandamis et al., (2000) challenged cells of *Salmonella* Typhimurium (10^3 CFU/ml) with oregano essential oil (0.03% w/v) in liquid media (TSB) and in gelatin-based system. This study demonstrated that the antimicrobial efficacy of oregano essential oil was reduced when the oil was added in the 3D model, in comparison with the liquid nutrient media. The decrease in the antibacterial activity was attributed to the microstructure, which limited the diffusion of the antimicrobial agent (P. Skandamis et al., 2000). The rheological properties of gelatin are significantly different from XG which is used in our study and that can impact the microbial dynamics (Costello et al., 2018). Additionally, on more rigid solid surfaces, the size of the bacterial colonies generally increases, due to a reduction in surface tension (Costello et al., 2018; Verheyen et al., 2019). Therefore, the colony itself can add an additional protection to the cells located in the centre of the colony, that cannot be in contact with the antimicrobial.

Further to the effects of the rheological properties, additional effects on the cell-antimicrobial component interactions can be induced by the structure/surface topography. As seen in Figure 3, the biphasic and triphasic 3D models developed in this study are highly pitted, with cavities and microchannels in comparison with the monophasic model (5% w/v XG) that has a smoother and much more homogeneous surface, as we previously reported (Costello et al., 2019). Such structural differences can affect the colony spreading/distribution and 3D

spatial organisation/growth. Increased cavities can lead to more space available for colonies to grow not only on the surface but within the 3D model's cavities, leading to potentially larger aggregates wherein only the periphery of the colony would be exposed to the antimicrobial compound (Costello et al., 2018, 2019; Skandamis & Jeanson, 2015). At the same time, colonies that can potentially grow within the surface cavities would have different access to nutrients and a higher level of self-induced acid stress that could lead to a higher tolerance to the antimicrobial via cross-protection mechanisms (Aspridou et al., 2014; Noriega et al., 2010; Velliou et al., 2012, 2013)

Further to structural and rheological properties the differences we see between our 3D systems can be also attributed to differences in their biochemical composition (presence of protein and fat). For example, when comparing the biphasic 3D model (XG/WPI) to the triphasic 3D model (XG/WPI/fat) in terms of rheological properties those are quite similar between them (Table 1, Figure A1 in appendix), indicating that the protein (WPI) is the main factor affecting the rheological behaviour of those models. The similarities in the microbial response to GSE on those two 3D models (Figure 2), also confirm that the rheological properties are a key factor affecting the antimicrobial action of GSE. However, when observing the surface topography, there are some (small) differences between the two 3D models (Figure 3). More specifically, the surface of the triphasic system is slightly more rough and irregular in comparison with the biphasic. Additionally, small craters on the surface of the triphasic 3D food model are visible (red arrows in Figure 3) representing fat rich areas. The presence of fat could affect the bioavailability of the antimicrobial, explaining why GSE had no effect at all against *L. monocytogenes* at 24 h of incubation (Figure 3f). Indeed, it has been reported in literature, that oils or proteins can affect the activity of natural antimicrobials. For example, Gutierrez et al (2008) studied the potential interaction between essential oils and basic food ingredients i.e., carbohydrate, protein and/or oil in simple *in vitro* models. They showed

485 reduced antimicrobial efficacy of essential oils when added in sunflower models. Conversely,
486 the antimicrobial activity of thyme and oregano oil was greater when added in the models with
487 high protein content (beef extract) (Gutierrez et al., 2008). However, other studies, have
488 observed reduced antimicrobial activity of essential oils added in presence milk proteins (Pol
489 et al., 2001; Smith-Palmer et al., 2001). In our case, the GSE are mainly composed by
490 proanthocyanidins which can form complexes with the WPI (milk protein) contained in our
491 biphasic and triphasic 3D models (Bisha et al., 2010; Li & Girard, 2023; Tang et al., 2021).
492 These complexes can enhance the stability and antioxidant activity of the phenolic compounds
493 but can lower the bioavailability to the bacterial cells. In other words, the complexes formed
494 by polyphenols and WPI limit the development of comparable complexes between phenolic
495 components and proteins or other components of the cell envelope, particularly the cell
496 membrane, which is considered one of the main mechanisms of inactivation of GSE.
497 Additionally, due to the WPI-phenolic compounds binding there are less phenolic compounds
498 available to penetrate the cell and cause further intracellular damage.

499 Overall, our findings indicate that GSE has great antimicrobial activity against surface
500 growth of *L. monocytogenes*, when added in liquid and simple single phase 3D model systems
501 of relatively low viscosity. However, when introducing structural and biochemical complexity,
502 i.e., adding protein or protein and oil, the antimicrobial activity of GSE is diminished, due to a
503 variety of factors, i.e., changes in rheology, structure-topography, biochemical composition
504 and/or their combination. Therefore, in order to use natural antimicrobials in complex food
505 products, the rheological, structural and biochemical properties of the food product need to be
506 taken into consideration.

507

3.2. Combined treatment of GSE and CAP against L. monocytogenes in monophasic and multiphasic 3D in vitro models.

As shown in the previous section (section 3.1), GSE caused a substantial decrease on the cell population of *L. monocytogenes* on our monophasic 3D models of relatively low viscosity (regardless of their viscosity) and only a slight disturbance in the microbial growth on our multiphasic, i.e., biphasic and triphasic 3D models. Combining GSE with another method/process, such as CAP, could result in higher microbial inactivation, leading to a more efficient and sustainable strategy to achieve microbial safety. CAP can have antimicrobial activity via destruction of the cell wall, DNA damage, lipid peroxidation and protein dysfunction (Guo et al., 2015; Niemira, 2012; Pankaj & Keener, 2017). Moreover, CAP could possibly reduce the metabolic activity of the cell resulting in the loss of the pathogenicity and interfere with the biofilm formation by destroying the extracellular polymeric substances (Bourke et al., 2018; Gilmore et al., 2018). As previously described (section 2.7), for the combined treatment of GSE and CAP, cells of *L. monocytogenes* were firstly inoculated on the surface of the monophasic and multiphasic 3D models containing 1% (w/v) GSE and incubated for 2 and 8 h. These time points were selected as they represent different levels of *L. monocytogenes* inactivation/growth disturbance by GSE, as shown in section 3.1 (Figure 2). After 2 h and 8 h of incubation, 3D models with or without GSE were treated with CAP for 2 min at 5 L/ min flow rate (primarily ozone composition) to assess the individual effect of CAP as well as the effect of CAP combined with GSE.

CAP (individual) treatment on monophasic and multiphasic 3D models

As shown in Figure 4 and Table 2, overall, the individual CAP treatment applied after 2 h and 8 h of incubation at 37 °C appears to have very little to no antimicrobial effect on the

surface of the monophasic XG based 3D *in vitro* models. When comparing the trend for the multiphasic 3D models, CAP treatment caused microbial inactivation for both 2 h and 8 h of incubation and for both the bi-phasic and the trip-phasic 3D model (Figure 5). The differences we observe between our models can be attributed to the stage of growth as well as the model structure and the spatial organisation of the cells on the models. More specifically, at 2 h of incubation, especially for the low viscosity monophasic models, i.e., 1.5 and 2.5% (w/v) XG, part of the bacterial population could be still planktonic and moving within less viscous areas of the surface (Skandamis & Jeanson, 2015; Skandamis & Nychas, 2012). The presence of such planktonic (sub-)populations would be more likely at earlier stages of incubation (2 h) as compared to later stages (8 h), where more colonies/cell aggregates are formed. Such a microenvironment (more likely at the earlier stages of incubation) is similar to a liquid system and, therefore, less favourable for microbial inactivation by CAP, as it hinders gas penetration and gas-cell interactions (Chizoba Ekezie et al., 2017; Costello et al., 2021a; Guo et al., 2015; Mandal et al., 2018; Smet et al., 2018; Surowsky et al., 2015). When the viscosity increases, i.e., for the 5% (w/v) XG monophasic 3D model (Figure 4) or for the biphasic and triphasic systems (Figure 5), as also discussed in the previous section, the colonies are more spread on the surface of the model, therefore leading to better CAP (gas)/colony contact and to higher CAP efficiency in causing inactivation (Costello et al., 2018). When comparing the impact of CAP on the microbial inactivation for early incubation (2h) as compared to the late incubation (8h) for the multiphasic models (Figure 5), the latter results in less microbial inactivation for both models. A possible explanation is that after 8 h, larger colonies have been formed along with early extracellular polymeric substances (EPS) overproduction, therefore there is additional protection for the cells located in the centre of the bigger colonies by hindering the diffusion of the reactive species (El Kadri et al., 2021; Flemming et al., 2016; Smet et al., 2019; Sun et al., 2022). Furthermore, as also discussed in section 3.1, the multiphasic models have

557 rougher surfaces, and this can be a hindering parameter for plasma treatment because it
558 provides a natural protection for the bacteria by attaching to the available cavities, especially
559 for large colonies at a later stages of growth (Surowsky et al., 2015).

560 CAP studies reported in literature to date for microbial inactivation are primarily conducted
561 in specific food products and consequently show very high variations of the magnitude of
562 microbial inactivation, i.e., ranging from no inhibition to several log (CFU/mL) reduction. This
563 is due to variations of the food properties such as the matrix, the water activity and pH, as well
564 as by the sensitivity of the bacterial strain and the initial cell concentration (Bahrami et al.,
565 2020; Chizoba Ekezie et al., 2017; Niakousari et al., 2018; Sharma et al., 2014) For example,
566 CAP induced microbial inactivation in meat products has been reported to range from 0.34-
567 6.52 log (Misra & Jo, 2017).

568 Collectively, the variation of the CAP antimicrobial potential reported to date in literature
569 with our results, show the importance of the conduction of fundamental studies in systems of
570 robustly controlled properties. Such studies will increase our understanding of the CAP action
571 in relation to cell-matrix and CAP-matrix interactions.

572

573 *Combined CAP and GSE treatment on monophasic and multiphasic 3D models*

574 In our study, the combination of GSE and CAP was generally more effective than the
575 individual treatments in all 3D models under study (Figures 4 & 5 and Table 2). As can be seen
576 in Figure 4, the microbial inactivation on the surface of the monophasic XG based systems was
577 0.43, 0.85 and 1.46 log, for 1.5%, 2.5% and 5% (w/v) XG respectively. These data demonstrate
578 that the microbial inhibition resulting from hurdle approach was greatest for the higher XG
579 concentration, similarly to the trend observed for the independent CAP treatment (Figure 4, see
580 also previous sub-section). A higher microbial inactivation when the hurdle approach, i.e., CAP

and GSE, was observed for both multiphasic 3D models as well, as compared to the individual CAP and GSE treatments (Figure 5). When comparing the microbial inactivation induced by the hurdle approach between monophasic (Figure 4) and multiphasic 3D models (Figure 5) a much lower inactivation is observed for the latter, which is expected, considering the very low impact of GSE on the microbial dynamics in those systems (Figures 2, 5, see also section 3.1). This, combined with the observation that CAP caused microbial inactivation as an individual treatment in both multiphasic 3D models and at levels similar to the combined CAP/GSE, indicates that the microbial inactivation imposed by the hurdle approach on the multiphasic 3D models can be mostly attributed to the action of the CAP treatment.

Overall, our results show that the combined treatment of GSE and CAP have a positive combined antimicrobial effect against *L. monocytogenes* in all the 3D models. However, the effect is much greater in the simple monophasic 3D models (Figure 4) as compared to the multiphasic models (Figure 5). To the best of our knowledge, there are no other studies to date combining GSE with CAP, however, there are previous studies investigating the combination of CAP with other natural antimicrobials. Those studies have also concluded that the hurdle approach was generally more effective than the individual treatments (Costello et al., 2021a; De la Ossa et al., 2021). For instance, Costello et al., (2021a) investigated the combined treatment of nisin (35 IU/ml, 30 min) and CAP (directly applied dielectric barrier discharge, 4 L/min helium and 40 mL/min oxygen, 30 min) against *L. innocua* in/on liquid and solid like 3D *in vitro* models (1.5% w/v XG) and observed greater microbial inactivation of the combined CAP/nisin treatment as compared to the individual treatments. De la Ossa et al., (2021), investigated the combined treatment of olive leaf extract (100 mg/ml total phenolic content) and CAP (using the same device employed in this study, 5 L/min, 1 min) in liquid nutrient broth against *L. innocua*. CAP combined with the olive leaf extract completely inactivated *L. innocua* after 6 h whereas no inhibition was noted by the individual treatments.

There are also some studies investigating the combined effect of CAP and natural antimicrobials in actual food products. The food products used by those studies were egg shells, dragon fruit and meat products on which different bacteria were inoculated such as *E.coli*, S. Typhimurium, *S. aureus* and *L. monocytogenes*. (Cui et al., 2016a, 2016b, 2017; Matan et al., 2015). Those studies have concluded that the hurdle approach using CAP with the respective natural antimicrobial per study had good synergistic effect. For example, Matan et al. in 2015, reported a synergistic effect of plasma (radio frequency 40W) and green tea extracts (5% w/v) against *E. coli, S. typhimurium,* and *L. monocytogenes* on the surface of freshly-cut dragon fruit (with a 10^6 CFU/ml initial microbial concentration). More specifically, plasma treatment was able to reduce the bacterial count by 1-1.5 logs, but the combined treatment with green tea extracts achieved total inactivation. In addition, when the dragon fruit was treated individually with green tea extracts no inhibition was shown (Matan et al., 2015). The same group also studied the synergistic effect of radio frequency plasma with essential oils from clove, sweet basil and lime in concentrations 0.5-2% (w/v) The most effective treatment was the combined treatment of plasma with clove oil (1% w/v), which led to a total microbial (*E. coli, S. typhimurium, S. aureus*) inhibition on eggshells (Matan et al., 2014). Similarly, Cui et al., (2016b) studied the effect of the combination of cold nitrogen plasma (400W) and thyme oil (0.05% w/v) against *S. typhimurium* and *S. enteritidis* on eggshells. The combination achieved a very high microbial reduction, i.e., below the detection limit 10 CFU/egg, that lasted for 14 days of storage (Cui et al., 2016b). The same year, Cui et al., (2016a) also showed that cold nitrogen plasma combined with *Helichrysum italicum* essential oil inhibit the population of *S. aureus* on food packaging. The microbial concentration decreased more than 5 logs, in contrast with individual treatments which caused only 2 logs reduction of the microbial concentration (Cui et al., 2016a).

Overall, considering the promising, yet contradictory results reported so far in literature regarding the combined treatment of CAP with natural antimicrobial compounds against various food-borne bacteria in different laboratory models or different food systems, along with the data we present in our study, it is evident that more research is required in this field. More specifically, normalisation or control of some parameters affecting the antimicrobial action – like the CAP composition (most importantly, RONS gas- and liquid-phase concentrations applied to targets), the type of natural antimicrobial, the structural and biochemical properties of the system used – will enable more accurate comparisons as well as the generation of more robust data to build accurate predictive microbiology tools for those novel processing approaches.

Conclusion

In this study we perform a novel systematic investigation of the antimicrobial activity of grape seed extracts (GSE), cold atmospheric plasma (CAP– in this case, a remote air plasma with an ozone-dominated RONS output) and their combination against *L. monocytogenes* on five different 3D in *vitro* models of varying rheological, structural, and biochemical composition. More specifically, we studied the microbial dynamics (as affected by GSE and CAP) in three monophasic Xanthan Gum (XG) based 3D models of relatively low viscosity (1.5%, 2.5% and 3% w/v XG) and in a biphasic XG/Whey Protein (WPI) and a triphasic XG/WPI/fat model.

A significant microbial inactivation (comparable to liquid broth) was achieved in presence of GSE on the surface of all monophasic models regardless of their viscosity. However, the GSE antimicrobial effect was diminished in the multiphasic systems, resulting to only a slight disturbance of the microbial growth. In contrast, CAP showed better antimicrobial potential on

654 the surface of the complex multiphasic models as compared to the monophasic models. When
655 combined, in a hurdle approach, GSE/CAP showed promising microbial inactivation potential
656 in all our 3D models, but less microbial inactivation in the structurally and rheologically
657 complex multiphasic models, with respect to the monophasic models. The level of inactivation
658 was also dependent on the duration of the GSE exposure.

659 Our findings shed light on the potential of GSE, CAP and their combination as a sustainable
660 antimicrobial strategy in the food industry. Furthermore, we show how the structural properties
661 and biochemical composition of our models can affect the antimicrobial efficacy of GSE, CAP
662 or their combination against *L. monocytogenes*. Future work should focus on testing this
663 combined treatment against Gram-negative bacteria which are known to be more resistant to
664 natural antimicrobials along with food storage and transportation temperatures. Furthermore,
665 generally, more comparative systematic studies of novel antimicrobial approaches (natural
666 antimicrobials, NTT, or both) in environment of robustly controlled structural and biochemical
667 properties will lead to the generation of more reliable predictive tools for the design of
668 industrial antimicrobial strategies.

669

670 **Acknowledgements**

671 This works was supported by the Doctoral College and the Department of Chemical and
672 Process Engineering of the University of Surrey, United Kingdom. The authors would like to
673 express their gratitude for the support provided by Kate Megan Reid (Lab Technician,
674 Nutritional Sciences), Anuska Mann (Lab Manager, Nutritional Sciences) and Ben Gibbons
675 (Experimental Officer, Department of Chemical and Process Engineering). E.V. is grateful to
676 the Royal Academy of Engineering for an Industrial Fellowship and to the Medical Research
677 Council UK for a New Investigator Research Grant (MR/V028553/1).

678 **References**

679 Ahn, J., Grün, I. U., & Mustapha, A. (2004). Antimicrobial and Antioxidant Activities of
680 Natural Extracts *in Vitro* and in Ground Beef. *Journal of Food Protection*, *67*(1), 148–
681 155. https://doi.org/10.4315/0362-028X-67.1.148

682 Ahn, J., Grün, I. U., & Mustapha, A. (2007). Effects of plant extracts on microbial growth,
683 color change, and lipid oxidation in cooked beef. *Food Microbiology*, *24*(1), 7–14.
684 https://doi.org/10.1016/j.fm.2006.04.006

685 Antwi, M., Theys, T. E., Bernaerts, K., Van Impe, J. F., & Geeraerd, A. H. (2008). Validation
686 of a model for growth of *Lactococcus lactis* and *Listeria innocua* in a structured gel
687 system: Effect of monopotassium phosphate. *International Journal of Food*
688 *Microbiology*, *125*(3), 320–329. https://doi.org/10.1016/j.ijfoodmicro.2008.04.014

689 Aryani, D. C., Zwietering, M. H., & den Besten, H. M. W. (2016). The effect of different
690 matrices on the growth kinetics and heat resistance of *Listeria monocytogenes* and
691 *Lactobacillus plantarum*. *International Journal of Food Microbiology*, *238*, 326–337.
692 https://doi.org/10.1016/j.ijfoodmicro.2016.09.012

693 Aspridou, Z., Moschakis, T., Biliaderis, C. G., & Koutsoumanis, K. P. (2014). Effect of the
694 substrate's microstructure on the growth of *Listeria monocytogenes*. *Food Research*
695 *International*, *64*, 683–691. https://doi.org/10.1016/j.foodres.2014.07.031

696 Bahrami, A., Moaddabdoost Baboli, Z., Schimmel, K., Jafari, S. M., & Williams, L. (2020).
697 Efficiency of novel processing technologies for the control of *Listeria monocytogenes* in
698 food products. *Trends in Food Science and Technology*, *96*(May 2019), 61–78.
699 https://doi.org/10.1016/j.tifs.2019.12.009

700 Baka, M., Noriega, E., Van Langendonck, K., & Van Impe, J. F. (2016). Influence of food

intrinsic complexity on *Listeria monocytogenes* growth in/on vacuum-packed model systems at suboptimal temperatures. *International Journal of Food Microbiology*, *235*, 17–27. https://doi.org/10.1016/j.ijfoodmicro.2016.06.029

Baka, M., Verheyen, D., Cornette, N., Vercruyssen, S., & Van Impe, J. F. (2017). *Salmonella Typhimurium* and *Staphylococcus aureus* dynamics in/on variable (micro)structures of fish-based model systems at suboptimal temperatures. *International Journal of Food Microbiology*, *240*, 32–39. https://doi.org/10.1016/j.ijfoodmicro.2016.08.004

Baydar, N.G., Özkan, G., & Sağdiç, O. (2004). Total phenolic contents and antibacterial activities of grape (*Vitis vinifera L.*) extracts. *Food Control*, *15*(5), 335–339. https://doi.org/10.1016/S0956-7135(03)00083-5

Baydar, N.G., Sagdic, O., Ozkan, G., & Cetin, S. (2006). Determination of antibacterial effects and total phenolic contents of grape (*Vitis vinifera L.*) seed extracts. *International Journal of Food Science and Technology*, *41*(7), 799–804. https://doi.org/10.1111/j.1365-2621.2005.01095.x

Begg, S. L. (2019). The role of metal ions in the virulence and viability of bacterial pathogens. *Biochemical Society Transactions*, *47*(1), 77–87. https://doi.org/10.1042/BST20180275

Bisha, B., Weinsetel, N., Brehm-Stecher, B. F., & Mendonca, A. (2010). Antilisterial effects of gravinol-S grape seed extract at low levels in aqueous media and its potential application as a produce wash. *Journal of Food Protection*, *73*(2), 266–273. https://doi.org/10.4315/0362-028X-73.2.266

Boons, K., Van Derlinden, E., Mertens, L., Peeters, V., & Van Impe, J. F. (2013). Effect of Immobilization and Salt Concentration on the Growth Dynamics of *Escherichia coli* K12 and *Salmonella* Typhimurium. *Journal of Food Science*, *78*(4), M567–M574.

https://doi.org/10.1111/1750-3841.12067

Bourke, P., Ziuzina, D., Boehm, D., Cullen, P. J., & Keener, K. (2018). The Potential of Cold Plasma for Safe and Sustainable Food Production. *Trends in Biotechnology*, *36*(6), 615–626. https://doi.org/10.1016/j.tibtech.2017.11.001

Chedea, V. S., & Pop, R. M. (2019). Total Polyphenols Content and Antioxidant DPPH Assays on Biological Samples. In *Polyphenols in Plants* (2nd ed., pp. 169–183). Elsevier. https://doi.org/10.1016/B978-0-12-813768-0.00011-6

Chizoba Ekezie, F. G., Sun, D. W., & Cheng, J. H. (2017). A review on recent advances in cold plasma technology for the food industry: Current applications and future trends. *Trends in Food Science and Technology*, *69*, 46–58. https://doi.org/10.1016/j.tifs.2017.08.007

Corrales, M., Han, J. H., & Tauscher, B. (2009). Antimicrobial properties of grape seed extracts and their effectiveness after incorporation into pea starch films. *International Journal of Food Science & Technology*, *44*(2), 425–433. https://doi.org/10.1111/j.1365-2621.2008.01790.x

Costa, M. M., Alfaia, C. M., Lopes, P. A., Pestana, J. M., & Prates, J. A. M. (2022). Grape By-Products as Feedstuff for Pig and Poultry Production. *Animals*, *12*(17), 2239. https://doi.org/10.3390/ani12172239

Costello, K. M., Gutierrez-Merino, J., Bussemaker, M., Ramaioli, M., Baka, M., Van Impe, J. F., & Velliou, E. G. (2018). Modelling the microbial dynamics and antimicrobial resistance development of *Listeria* in viscoelastic food model systems of various structural complexities. *International Journal of Food Microbiology*, *286*(February), 15–30. https://doi.org/10.1016/j.ijfoodmicro.2018.07.011

748 Costello, K. M., Gutierrez-Merino, J., Bussemaker, M., Smet, C., Van Impe, J. F., & Velliou,
749 E. G. (2019). A multi-scale analysis of the effect of complex viscoelastic models on
750 *Listeria* dynamics and adaptation in co-culture systems. *AIChE Journal*, *66*(1), 1–15.
751 https://doi.org/10.1002/aic.16761

752 Costello, K. M., Smet, C., Gutierrez-Merino, J., Bussemaker, M., Van Impe, J. F., & Velliou,
753 E. G. (2021a). The impact of food model system structure on the inactivation of *Listeria*
754 *innocua* by cold atmospheric plasma and nisin combined treatments. *International*
755 *Journal of Food Microbiology*, *337*(August 2020), 108948.
756 https://doi.org/10.1016/j.ijfoodmicro.2020.108948

757 Costello, K. M., Velliou, E.G., Gutierrez-Merino, J., Smet, C., Kadri, H. El, Impe, J. F. Van,
758 & Bussemaker, M. (2021b). The effect of ultrasound treatment in combination with
759 nisin on the inactivation of *Listeria innocua* and *Escherichia coli*. *Ultrasonics*
760 *Sonochemistry*, *79*(September), 105776. https://doi.org/10.1016/j.ultsonch.2021.105776

761 Cui, H., Li, W., Li, C., & Lin, L. (2016a). Synergistic effect between *Helichrysum italicum*
762 essential oil and cold nitrogen plasma against Staphylococcus aureus biofilms on
763 different food-contact surfaces. *International Journal of Food Science and Technology*,
764 *51*(11), 2493–2501. https://doi.org/10.1111/ijfs.13231

765 Cui, H., Ma, C., Li, C., & Lin, L. (2016b). Enhancing the antibacterial activity of thyme oil
766 against *Salmonella* on eggshell by plasma-assisted process. *Food Control*, *70*, 183–190.
767 https://doi.org/10.1016/j.foodcont.2016.05.056

768 Cui, H., Ma, C., & Lin, L. (2016c). Synergetic antibacterial efficacy of cold nitrogen plasma
769 and clove oil against *Escherichia coli* O157:H7 biofilms on lettuce. *Food Control*, *66*,
770 8–16. https://doi.org/10.1016/j.foodcont.2016.01.035

771 Cui, H., Wu, J., Li, C., & Lin, L. (2017). Promoting anti-listeria activity of lemongrass oil on

772 pork loin by cold nitrogen plasma assist. *Journal of Food Safety*, *37*(2), e12316.
773 https://doi.org/10.1111/jfs.12316

774 Das, N., Tripathi, N., Basu, S., Bose, C., Maitra, S., & Khurana, S. (2015). Progress in the
775 development of gelling agents for improved culturability of microorganisms. *Frontiers*
776 *in Microbiology*, *6*(July), 1–7. https://doi.org/10.3389/fmicb.2015.00698

777 Dávila-Aviña, J. E., Solís-Soto, L. Y., Rojas-Verde, G., & Salas, N. A. (2015). Sustainability
778 and Challenges of Minimally Processed Foods. In *Food Engineering Series* (Issue June,
779 pp. 279–295). https://doi.org/10.1007/978-3-319-10677-9_12

780 De la Ossa, J. G., El Kadri, H., Gutierrez-Merino, J., Wantock, T., Harle, T., Seggiani, M.,
781 Danti, S., Di Stefano, R., & Velliou, E. (2021). Combined Antimicrobial Effect of Bio-
782 Waste Olive Leaf Extract and Remote Cold Atmospheric Plasma Effluent. *Molecules*,
783 *26*(7), 1890. https://doi.org/10.3390/molecules26071890

784 Delgado Adámez, J., Gamero Samino, E., Valdés Sánchez, E., & González-Gómez, D.
785 (2012). *In vitro* estimation of the antibacterial activity and antioxidant capacity of
786 aqueous extracts from grape-seeds (*Vitis vinifera L.*). *Food Control*, *24*(1–2), 136–141.
787 https://doi.org/10.1016/j.foodcont.2011.09.016

788 Deng, Q., & Zhao, Y. (2011). Physicochemical, nutritional, and antimicrobial properties of
789 wine grape (cv. Merlot) pomace extract-based films. *Journal of Food Science*, *76*(3),
790 E309–E317. https://doi.org/10.1111/j.1750-3841.2011.02090.x

791 El Kadri, H., Costello, K. M., Thomas, P., Wantock, T., Sandison, G., Harle, T., Fabris, A.
792 L., Gutierrez-Merino, J., & Velliou, E. G. (2021). The antimicrobial efficacy of remote
793 cold atmospheric plasma effluent against single and mixed bacterial biofilms of varying
794 age. *Food Research International*, *141*(January), 110126.
795 https://doi.org/10.1016/j.foodres.2021.110126

796 Flemming, H.-C., Wingender, J., Szewzyk, U., Steinberg, P., Rice, S. A., & Kjelleberg, S.
797 (2016). Biofilms: an emergent form of bacterial life. *Nature Reviews Microbiology*,
798 *14*(9), 563–575. https://doi.org/10.1038/nrmicro.2016.94

799 Garcia-Gonzalez, L., Geeraerd, A. H., Elst, K., Van Ginneken, L., Van Impe, J. F., &
800 Devlieghere, F. (2009). Influence of type of microorganism, food ingredients and food
801 properties on high-pressure carbon dioxide inactivation of microorganisms.
802 *International Journal of Food Microbiology*, *129*(3), 253–263.
803 https://doi.org/10.1016/j.ijfoodmicro.2008.12.005

804 Gilmore, B. F., Flynn, P. B., O'Brien, S., Hickok, N., Freeman, T., & Bourke, P. (2018).
805 Cold Plasmas for Biofilm Control: Opportunities and Challenges. *Trends in*
806 *Biotechnology*, *36*(6), 627–638. https://doi.org/10.1016/j.tibtech.2018.03.007

807 Guo, J., Huang, K., & Wang, J. (2015). Bactericidal effect of various non-thermal plasma
808 agents and the influence of experimental conditions in microbial inactivation: A review.
809 *Food Control*, *50*, 482–490. https://doi.org/10.1016/j.foodcont.2014.09.037

810 Gutierrez, J., Barry-Ryan, C., & Bourke, P. (2008). The antimicrobial efficacy of plant
811 essential oil combinations and interactions with food ingredients. *International Journal*
812 *of Food Microbiology*, *124*(1), 91–97. https://doi.org/10.1016/j.ijfoodmicro.2008.02.028

813 Karina, P., Julio, C., Leda, G., & Noemi, Z. (2011). Behavior of *Listeria monocytogenes*
814 type1 355/98 (85) in meat emulsions as affected by temperature, pH, water activity, fat
815 and microbial preservatives. *Food Control*, *22*(10), 1573–1581.
816 https://doi.org/10.1016/j.foodcont.2011.03.013

817 Karnopp, A. R., Margraf, T., Maciel, L. G., Santos, J. S., & Granato, D. (2017). Chemical
818 composition, nutritional and in vitro functional properties of by-products from the
819 Brazilian organic grape juice industry. *International Food Research Journal*, *24*(1),

207–214.

Katalinić, V., Možina, S. S., Skroza, D., Generalić, I., Abramovič, H., Miloš, M., Ljubenkov, I., Piskernik, S., Pezo, I., Terpinc, P., & Boban, M. (2010). Polyphenolic profile, antioxidant properties and antimicrobial activity of grape skin extracts of 14 *Vitis vinifera* varieties grown in Dalmatia (Croatia). *Food Chemistry*, *119*(2), 715–723. https://doi.org/10.1016/j.foodchem.2009.07.019

Khan, I., Tango, C. N., Miskeen, S., Lee, B. H., & Oh, D.-H. (2017). Hurdle technology: A novel approach for enhanced food quality and safety – A review. *Food Control*, *73*, 1426–1444. https://doi.org/10.1016/j.foodcont.2016.11.010

Kitsiou, M., Purk, L., Gutierrez-Merino, J., Karatzas, K. A., Klymenko, O. V., & Velliou, E. (2023). A Systematic Quantitative Determination of the Antimicrobial Efficacy of Grape Seed Extract against Foodborne Bacterial Pathogens. *Foods*, *12*(5), 929. https://doi.org/10.3390/foods12050929

Leistner, L. (2000). Basic aspects of food preservation by hurdle technology. *International Journal of Food Microbiology*, *55*(1–3), 181–186. https://doi.org/10.1016/S0168-1605(00)00161-6

Li, N., & Girard, A. L. (2023). Impact of pH and temperature on whey protein-proanthocyanidin interactions and foaming properties. *Food Hydrocolloids*, *134*(August 2022), 108100. https://doi.org/10.1016/j.foodhyd.2022.108100

Makariti, I. P., Grivokostopoulos, N. C., & Skandamis, P. N. (2021). Effect of oxygen availability and pH on adaptive acid tolerance response of immobilized *Listeria monocytogenes* in structured growth media. *Food Microbiology*, *99*(February), 103826. https://doi.org/10.1016/j.fm.2021.103826

Mandal, R., Singh, A., & Pratap Singh, A. (2018). Recent developments in cold plasma decontamination technology in the food industry. *Trends in Food Science and Technology*, *80*(November 2017), 93–103. https://doi.org/10.1016/j.tifs.2018.07.014

Matan, N., Nisoa, M., & Matan, N. (2014). Antibacterial activity of essential oils and their main components enhanced by atmospheric RF plasma. *Food Control*, *39*(1), 97–99. https://doi.org/10.1016/j.foodcont.2013.10.030

Matan, N., Puangjinda, K., Phothisuwan, S., & Nisoa, M. (2015). Combined antibacterial activity of green tea extract with atmospheric radio-frequency plasma against pathogens on fresh-cut dragon fruit. *Food Control*, *50*, 291–296. https://doi.org/10.1016/j.foodcont.2014.09.005

Mertens, L., Geeraerd, A. H., Dang, T. D. T., Vermeulen, A., Serneels, K., Van Derlinden, E., Cappuyns, A. M., Moldenaers, P., Debevere, J., Devlieghere, F., & Van Impe, J. F. (2009). Design of an Experimental Viscoelastic Food Model System for Studying *Zygosaccharomyces bailii* Spoilage in Acidic Sauces. *Applied and Environmental Microbiology*, *75*(22), 7060–7069. https://doi.org/10.1128/AEM.01045-09

Millan-Sango, D., McElhatton, A., & Valdramidis, V. P. (2015). Determination of the efficacy of ultrasound in combination with essential oil of oregano for the decontamination of *Escherichia coli* on inoculated lettuce leaves. *Food Research International*, *67*, 145–154. https://doi.org/10.1016/j.foodres.2014.11.001

Misra, N. N., & Jo, C. (2017). Applications of cold plasma technology for microbiological safety in meat industry. *Trends in Food Science and Technology*, *64*, 74–86. https://doi.org/10.1016/j.tifs.2017.04.005

Mosqueda-Melgar, J., Raybaudi-Massilia, R. M., & Martín-Belloso, O. (2008). Combination of high-intensity pulsed electric fields with natural antimicrobials to inactivate

pathogenic microorganisms and extend the shelf-life of melon and watermelon juices. *Food Microbiology*, *25*(3), 479–491. https://doi.org/10.1016/j.fm.2008.01.002

Niakousari, M., Gahruie, H. H., Razmjooei, M., Roohinejad, S., & Greiner, R. (2018). Effects of innovative processing technologies on microbial targets based on food categories: Comparing traditional and emerging technologies for food preservation. In *Innovative technologies for food preservation: Inactivation of spoilage and pathogenic microorganisms*. Elsevier Inc. https://doi.org/10.1016/B978-0-12-811031-7.00005-4

Niemira, B. A. (2012). Cold plasma decontamination of foods *. *Annual Review of Food Science and Technology*, *3*(1), 125–142. https://doi.org/10.1146/annurev-food-022811-101132

Noriega, E., Laca, A., & Díaz, M. (2010). Development of a structure-based model for the competitive growth of *Listeria innocua* in minced chicken breasts. *International Journal of Food Microbiology*, *142*(1–2), 44–52. https://doi.org/10.1016/j.ijfoodmicro.2010.05.025

Noriega, E., Velliou, E. G., Van Derlinden, E., Mertens, L., & Van Impe, J. F. M. (2014). Role of growth morphology in the formulation of NaCl-based selective media for injury detection of *Escherichia coli* , *Salmonella* Typhimurium and *Listeria innocua*. *Food Research International*, *64*, 402–411. https://doi.org/10.1016/j.foodres.2014.06.047

Oliveira, D. A., Salvador, A. A., Smânia, A., Smânia, E. F. A., Maraschin, M., & Ferreira, S. R. S. (2013). Antimicrobial activity and composition profile of grape (*Vitis vinifera*) pomace extracts obtained by supercritical fluids. *Journal of Biotechnology*, *164*(3), 423–432. https://doi.org/10.1016/j.jbiotec.2012.09.014

Pankaj, S. K., & Keener, K. M. (2017). Cold plasma: background, applications and current trends. *Current Opinion in Food Science*, *16*, 49–52.

https://doi.org/10.1016/j.cofs.2017.07.008

Pankaj, S. K., Wan, Z., & Keener, K. M. (2018). Effects of cold plasma on food quality: A review. *Foods*, *7*(1). https://doi.org/10.3390/foods7010004

Patange, A., O'Byrne, C., Boehm, D., Cullen, P. J., Keener, K., & Bourke, P. (2019). The Effect of Atmospheric Cold Plasma on Bacterial Stress Responses and Virulence Using *Listeria monocytogenes* Knockout Mutants. *Frontiers in Microbiology*, *10*(December), 1–12. https://doi.org/10.3389/fmicb.2019.02841

Peleg, M. (2020). The Hurdle Technology Metaphor Revisited. *Food Engineering Reviews*, *12*(3), 309–320. https://doi.org/10.1007/s12393-020-09218-z

Pereira, R. N., & Vicente, A. A. (2010). Environmental impact of novel thermal and non-thermal technologies in food processing. *Food Research International*, *43*(7), 1936–1943. https://doi.org/10.1016/j.foodres.2009.09.013

Piyasena, P., Mohareb, E., & McKellar, R. C. (2003). Inactivation of microbes using ultrasound: A review. *International Journal of Food Microbiology*, *87*(3), 207–216. https://doi.org/10.1016/S0168-1605(03)00075-8

Pol, I. E., Mastwijk, H. C., Slump, R. A., Popa, M. E., & Smid, E. J. (2001). Influence of Food Matrix on Inactivation of *Bacillus cereus* by Combinations of Nisin, Pulsed Electric Field Treatment, and Carvacrol. *Journal of Food Protection*, *64*(7), 1012–1018. https://doi.org/10.4315/0362-028X-64.7.1012

Polyakov, V. I., Grinberg, V. Y., & Tolstoguzov, V. B. (1997). Thermodynamic incompatibility of proteins. *Food Hydrocolloids*, *11*(2), 171–180. https://doi.org/10.1016/S0268-005X(97)80024-0

Sabater, C., Ruiz, L., Delgado, S., Ruas-Madiedo, P., & Margolles, A. (2020). Valorization of

914 Vegetable Food Waste and By-Products Through Fermentation Processes. *Frontiers in*
915 *Microbiology*, *11*(October), 1–11. https://doi.org/10.3389/fmicb.2020.581997

916 Sagdic, O., Ozturk, I., Yilmaz, M. T., & Yetim, H. (2011). Effect of Grape Pomace Extracts
917 Obtained from Different Grape Varieties on Microbial Quality of Beef Patty. *Journal of*
918 *Food Science*, *76*(7), M515–M521. https://doi.org/10.1111/j.1750-3841.2011.02323.x

919 Sharma, M., Usmani, Z., Gupta, V. K., & Bhat, R. (2021). Valorization of fruits and
920 vegetable wastes and by-products to produce natural pigments. *Critical Reviews in*
921 *Biotechnology*, *41*(4), 535–563. https://doi.org/10.1080/07388551.2021.1873240

922 Sharma, P., Bremer, P., Oey, I., & Everett, D. W. (2014). Bacterial inactivation in whole milk
923 using pulsed electric field processing. *International Dairy Journal*, *35*(1), 49–56.
924 https://doi.org/10.1016/j.idairyj.2013.10.005

925 Shrikhande, A. J. (2000). Wine by-products with health benefits. *Food Research*
926 *International*, *33*(6), 469–474. https://doi.org/10.1016/S0963-9969(00)00071-5

927 Silva, V., Igrejas, G., Falco, V., Santos, T. P., Torres, C., Oliveira, A. M. P., Pereira, J. E.,
928 Amaral, J. S., & Poeta, P. (2018). Chemical composition, antioxidant and antimicrobial
929 activity of phenolic compounds extracted from wine industry by-products. *Food*
930 *Control*, *92*(May), 516–522. https://doi.org/10.1016/j.foodcont.2018.05.031

931 Silván, J. M., Mingo, E., Hidalgo, M., de Pascual-Teresa, S., Carrascosa, A. V., & Martinez-
932 Rodriguez, A. J. (2013). Antibacterial activity of a grape seed extract and its fractions
933 against *Campylobacter* spp. *Food Control*, *29*(1), 25–31.
934 https://doi.org/10.1016/j.foodcont.2012.05.063

935 Sivarooban, T., Hettiarachchy, N. S., & Johnson, M. G. (2007). Inhibition of *Listeria*
936 *monocytogenes* using nisin with grape seed extract on turkey frankfurters stored at 4 and

10°C. *Journal of Food Protection*, *70*(4), 1017–1020. https://doi.org/10.4315/0362-028X-70.4.1017

Skandamis, P. N., & Jeanson, S. (2015). Colonial vs. planktonic type of growth: mathematical modeling of microbial dynamics on surfaces and in liquid, semi-liquid and solid foods. *Frontiers in Microbiology*, *6*(OCT), 1–9. https://doi.org/10.3389/fmicb.2015.01178

Skandamis, P. N., & Nychas, G.-J. E. (2012). Quorum Sensing in the Context of Food Microbiology. *Applied and Environmental Microbiology*, *78*(16), 5473–5482. https://doi.org/10.1128/AEM.00468-12

Skandamis, P.N., Tsigarida, E., & Nychas, G. J. E. (2000). Ecophysiological attributes of *Salmonella* Typhimurium in liquid culture and within a gelatin gel with or without the addition of oregano essential oil. *World Journal of Microbiology and Biotechnology*, *16*(1), 31–35. https://doi.org/10.1023/A:1008934020409

Smet, C., Noriega, E., Rosier, F., Walsh, J. L., Valdramidis, V. P., & Van Impe, J. F. (2017). Impact of food model (micro)structure on the microbial inactivation efficacy of cold atmospheric plasma. *International Journal of Food Microbiology*, *240*, 47–56. https://doi.org/10.1016/j.ijfoodmicro.2016.07.024

Smet, Cindy, Baka, M., Dickenson, A., Walsh, J. L., Valdramidis, V. P., & Van Impe, J. F. (2018). Antimicrobial efficacy of cold atmospheric plasma for different intrinsic and extrinsic parameters. *Plasma Processes and Polymers*, *15*(2), 1700048. https://doi.org/10.1002/ppap.201700048

Smet, Cindy, Govaert, M., Kyrylenko, A., Easdani, M., Walsh, J. L., & Van Impe, J. F. (2019). Inactivation of single strains of *Listeria monocytogenes* and *Salmonella* Typhimurium planktonic cells biofilms with plasma activated liquids. *Frontiers in*

961 *Microbiology*, *10*(JULY), 1–15. https://doi.org/10.3389/fmicb.2019.01539

962 Smith-Palmer, A., Stewart, J., & Fyfe, L. (2001). The potential application of plant essential
963 oils as natural food preservatives in soft cheese. *Food Microbiology*, *18*(4), 463–470.
964 https://doi.org/10.1006/fmic.2001.0415

965 Sun, J., Huang, L., Sun, Z., Wang, D., Liu, F., Du, L., & Wang, D. (2022). Combination of
966 ultrasound and chlorogenic acid for inactivation of planktonic and biofilm cells of
967 *Pseudomonas fluorescens*. *Food Research International*, *155*(February), 111009.
968 https://doi.org/10.1016/j.foodres.2022.111009

969 Sunil, Chauhan, N., Singh J.,, Chandra, S., Chaudhary V., & Vikrant Kumar N. (2018).
970 "Non-thermal techniques: Application in food industries" A review. *Journal of*
971 *Pharmacognosy and Phytochemistry*, *7(5)*(5), 1507–1518.
972 http://www.phytojournal.com/archives/2018/vol7issue5/PartZ/7-4-659-545.pdf

973 Surowsky, B., Schlüter, O., & Knorr, D. (2015). Interactions of Non-Thermal Atmospheric
974 Pressure Plasma with Solid and Liquid Food Systems: A Review. *Food Engineering*
975 *Reviews*, *7*(2), 82–108. https://doi.org/10.1007/s12393-014-9088-5

976 Tang, C., Tan, B., & Sun, X. (2021). Elucidation of Interaction between Whey Proteins and
977 Proanthocyanidins and Its Protective Effects on Proanthocyanidins during *In-Vitro*
978 Digestion and Storage. *Molecules*, *26*(18), 5468.
979 https://doi.org/10.3390/molecules26185468

980 Tewari, G., & Juneja, V. K. (2007). *Advances in Thermal and Non-Thermal Food*
981 *Preservation* (G. Tewari & V. K. Juneja (eds.)). Blackwell Publishing.
982 https://doi.org/10.1002/9780470277898

983 Thirumdas, R., Sarangapani, C., & Annapure, U. S. (2014). Cold Plasma: A novel Non-

Thermal Technology for Food Processing. *Food Biophysics*, *10*(1), 1–11. https://doi.org/10.1007/s11483-014-9382-z

Vandekinderen, I., Devlieghere, F., Van Camp, J., Kerkaert, B., Cucu, T., Ragaert, P., De Bruyne, J., & De Meulenaer, B. (2009). Effects of food composition on the inactivation of foodborne microorganisms by chlorine dioxide. *International Journal of Food Microbiology*, *131*(2–3), 138–144. https://doi.org/10.1016/j.ijfoodmicro.2009.02.004

Velliou, E.G., Noriega, E., Van Derlinden, E., Mertens, L., Boons, K., Geeraerd, A. H., Devlieghere, F., & Van Impe, J. F. (2013). The effect of colony formation on the heat inactivation dynamics of *Escherichia coli* K12 and *Salmonella* Typhimurium. *Food Research International*, *54*(2), 1746–1752. https://doi.org/10.1016/j.foodres.2013.09.009

Velliou, E.G., Van Derlinden, E., Cappuyns, A. M., Aerts, D., Nikolaidou, E., Geeraerd, A. H., Devlieghere, F., & Van Impe, J. F. (2011). Quantification of the influence of trimethylamine-N-oxide (TMAO) on the heat resistance of *Escherichia coli* K12 at lethal temperatures. *Letters in Applied Microbiology*, *52*(2), 116–122. https://doi.org/10.1111/j.1472-765X.2010.02974.x

Velliou, E.G., Van Derlinden, E., Cappuyns, A. M., Geeraerd, A. H., Devlieghere, F., & Van Impe, J. F. (2012). Heat inactivation of *Escherichia coli* K12 MG1655: Effect of microbial metabolites and acids in spent medium. *Journal of Thermal Biology*, *37*(1), 72–78. https://doi.org/10.1016/j.jtherbio.2011.11.001

Velliou, E.G., Van Derlinden, E., Cappuyns, A. M., Nikolaidou, E., Geeraerd, A. H., Devlieghere, F., & Van Impe, J. F. (2011). Towards the quantification of the effect of acid treatment on the heat tolerance of *Escherichia coli* K12 at lethal temperatures. *Food Microbiology*, *28*(4), 702–711. https://doi.org/10.1016/j.fm.2010.06.007

1008 Velliou, E.G., Van Derlinden, E., Cappuyns, A. M., Goossens, J., Geeraerd, A. H.,
1009 Devlieghere, F., & Van Impe, J. F. (2011). Heat adaptation of *Escherichia coli* K12:
1010 Effect of acid and glucose. *Procedia Food Science*, *1*, 987–993.
1011 https://doi.org/10.1016/j.profoo.2011.09.148

1012 Verheyen, D., Govaert, M., Seow, T. K., Ruvina, J., & Mukherjee, V. (2020). The Complex
1013 Effect of Food Matrix Fat Content on Thermal Inactivation of *Listeria monocytogenes :*
1014 *Case Study in Emulsion and Gelled Emulsion Model Systems*. *10*(January), 2–3.
1015 https://doi.org/10.3389/fmicb.2019.03149

1016 Verheyen, D., Xu, X. M., Govaert, M., Baka, M., Skåra, T., & Van Impe, J. F. (2019). Food
1017 Microstructure and Fat Content Affect Growth Morphology, Growth Kinetics, and
1018 Preferred Phase for Cell Growth of *Listeria monocytogenes* in Fish-Based Model
1019 Systems. *Applied and Environmental Microbiology*, *85*(16), 1–18.
1020 https://doi.org/10.1128/AEM.00707-19

1021 Wang, X., Devlieghere, F., Geeraerd, A., & Uyttendaele, M. (2017). Thermal inactivation
1022 and sublethal injury kinetics of *Salmonella enterica* and *Listeria monocytogenes* in broth
1023 versus agar surface. *International Journal of Food Microbiology*, *243*, 70–77.
1024 https://doi.org/10.1016/j.ijfoodmicro.2016.12.008

1025 Xu, Y., Burton, S., Kim, C., & Sismour, E. (2016). Phenolic compounds, antioxidant, and
1026 antibacterial properties of pomace extracts from four virginia-grown grape varieties.
1027 *Food Science and Nutrition*, *4*(1), 125–133. https://doi.org/10.1002/fsn3.264

1028 Zhao, X., Chen, L., Wu, J., He, Y., & Yang, H. (2020). Elucidating antimicrobial mechanism
1029 of nisin and grape seed extract against *Listeria monocytogenes* in broth and on shrimp
1030 through NMR-based metabolomics approach. *International Journal of Food*
1031 *Microbiology*, *319*(August 2019), 108494.

https://doi.org/10.1016/j.ijfoodmicro.2019.108494

Table legends

Table 1. Average values for storage modulus *G'*, loss modulus *G"*, *tanδ* and their associated average standard deviations for the 5% monophasic XG and the multiphasic 3D models at 37 °C.

Table 2. Summary of findings on the combined treatment of GSE and CAP against *L. monocytogenes.*

Figure legends

Figure 1. A flow diagram of the CAP set-up.

Figure 2: Inactivation dynamics of *L. monocytogenes* 10403S WT (a) in liquid broth (TSBYE), on the surface of monophasic 3D models containing (b) 1.5% XG (c) 2.5% XG (d) 5% XG (w/v) and on the surface of (e) biphasic 3D models (5% w/v XG/ 10% w/v WPI), and (f) triphasic 3D models (5% w/v XG/ 10% w/v WPI/ 10% v/v fat). In all plots, (●) control (w/o GSE), (**x**) 1% (w/v) GSE. Each time point represents the average of three independent experiments with two technical replicates per experiment. Error bars show standard deviation.

***Figure 3*:** SEM images of the structure of the (a) Biphasic 3D model (5% w/v XG and 10% w/v WPI), (b) Triphasic 3D model (5% w/v XG, 10% w/v WPI and 10% v/v fat). The red arrows indicate the fat rich areas of the 3D triphasic model.

***Figure 4*:** Inactivation of *L. monocytogenes* 10403S WT inoculated on the surface of monophasic 3D models with 1.5%, 2.5% and 5% (w/v) XG, incubated for 2 h and 8 h at 37 °C. In all plots, (■) control, (■) CAP treatment for 2 minutes at a flow rate of 5 L/min (primarily ozone composition), (■) 1% (w/v) GSE incorporated in the 3D models, (■) Combination of 1% (w/v) GSE and CAP treatment for 2 min. Each bar represents the average of three independent experiments with two technical replicates per experiments. Error bars show standard deviation. Connecting lines with asterisks indicate significant differences between control and treated samples (* if $0.01<p \leq 0.05$, ** if $0.001< p \leq 0.01$, *** if $p \leq 0.001$)

***Figure 5*:** Inactivation of *L. monocytogenes* 10403S WT inoculated on the surface of biphasic 3D models (5% w/v XG, 10% w/v WPI) and triphasic 3D models (5% w/v XG, 10% w/v WPI, 10% v/v fat), incubated for 2 h and 8 h at 37 °C. In all plots, (■) control, (■) 2'CAP treatment at 5 L/min, (■) 1% (w/v) GSE incorporated in the 3D model, (■) Combination of 1% (w/v) GSE and CAP treatment for 2 minutes at a flow rate of 5 L/min. Each bar represents the average

of three independent experiments with two technical replicates per experiments. Error bars show standard deviation. Connecting lines with asterisks indicate significant differences between control and treated samples (* if $0.01<p \leq 0.05$, ** if $0.001< p \leq 0.01$, *** if $p \leq 0.001$)

List of Tables

Table 1

Food model	Temperature	G'	G''	*tanδ* (= G''/ G')
Monophasic* 5% XG	37 °C	376 ± 74.5	61 ± 13.9	0.167 ± 0.004
Biphasic 5% XG + 10% WPI	37 °C	1961 ± 84.1	399 ± 12.6	0.210 ± 0.005
Triphasic 5% XG + 10% WPI + 10% fat	37 °C	2159 ± 79.3	407 ± 10.9	0.194 ± 0.004

*from Costello *et al.*, 2018

1129 **Table 2**

Type of 3D model		CAP	GSE	GSE + CAP
Monophasic 1.5% XG	2 h	no changes	microbial inactivation (<1 log CFU/ml)	microbial inactivation (<1 log CFU/ml)
	8 h	no changes	microbial inactivation (>1 log CFU/ml)	microbial inactivation (>1 log CFU/ml)
Monophasic 2.5% XG	2 h	microbial inactivation (<1 log CFU/ml)	microbial inactivation (<1 log CFU/ml)	microbial inactivation (<1 log CFU/ml)
	8 h	microbial inactivation (<1 log CFU/ml)	microbial inactivation (>1 log CFU/ml)	microbial inactivation (>1 log CFU/ml)
Monophasic 5% XG	2 h	microbial inactivation (<1 log CFU/ml)	microbial inactivation (<1 log CFU/ml)	microbial inactivation (>1 log CFU/ml)
	8 h	microbial inactivation (<1 log CFU/ml)	microbial inactivation (>1 log CFU/ml)	microbial inactivation (>1 log CFU/ml)
Biphasic 5% XG + 10% WPI	2 h	microbial inactivation (>1 log CFU/ml)	microbial inactivation (<1 log CFU/ml)	microbial inactivation (>1 log CFU/ml)
	8 h	microbial inactivation (<1 log CFU/ml)	microbial inactivation (<1 log CFU/ml)	microbial inactivation (<1 log CFU/ml)
Triphasic 5% XG + 10% WPI + 10% fat	2 h	microbial inactivation (<1 log CFU/ml)	no changes	microbial inactivation (<1 log CFU/ml)
	8 h	microbial inactivation (<1 log CFU/ml)	microbial inactivation (<1 log CFU/ml)	microbial inactivation (<1 log CFU/ml)

1130

1131

1132

1133

1134

List of Figures

Figure 1

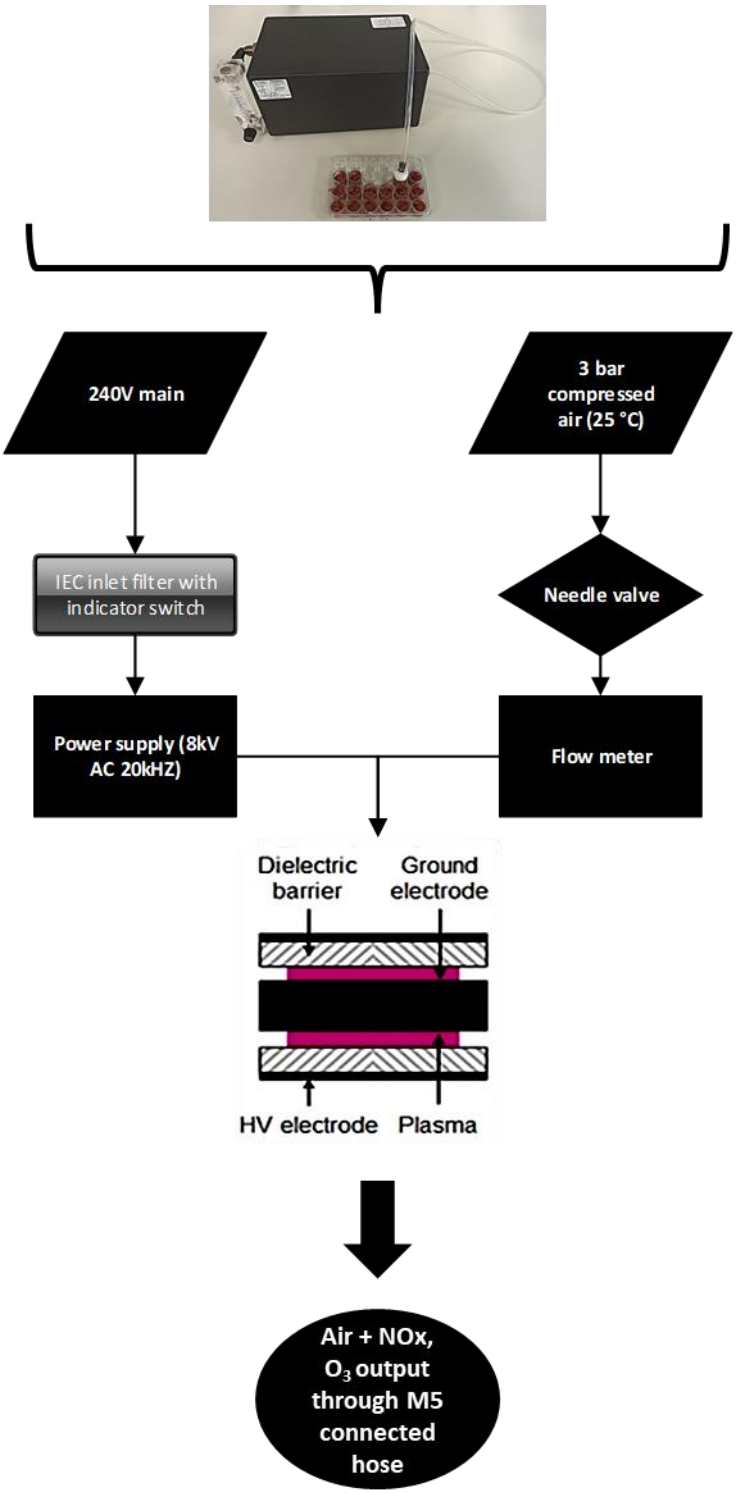

Figure 2

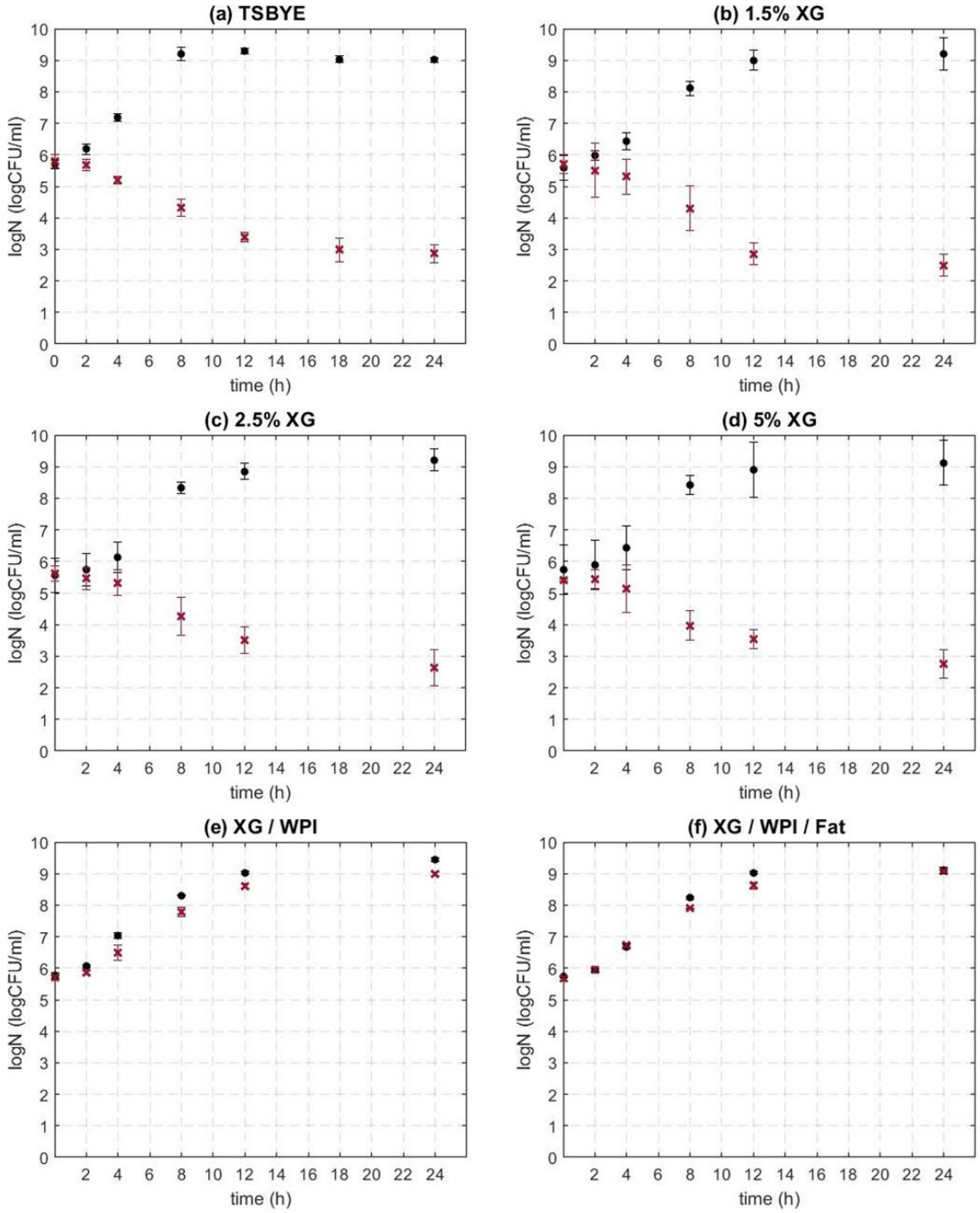
(a) TSBYE
(b) 1.5% XG
(c) 2.5% XG
(d) 5% XG
(e) XG / WPI
(f) XG / WPI / Fat
logN (logCFU/ml)
time (h)

Figure 3

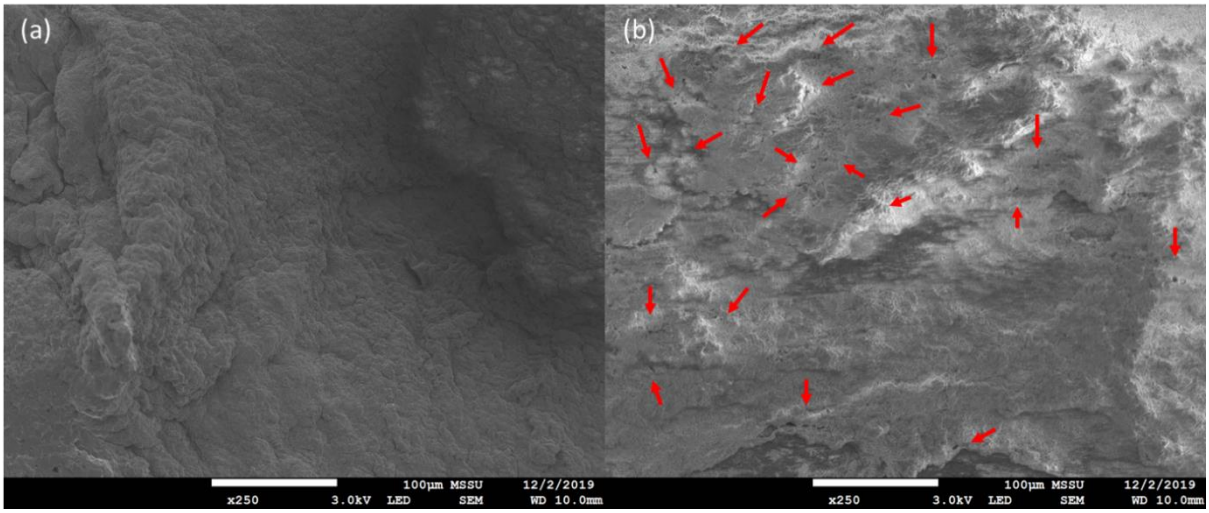
(a)
(b)
100µm MSSU 12/2/2019
x250 3.0kV LED SEM WD 10.0mm
100µm MSSU 12/2/2019
x250 3.0kV LED SEM WD 10.0mm

Figure 4

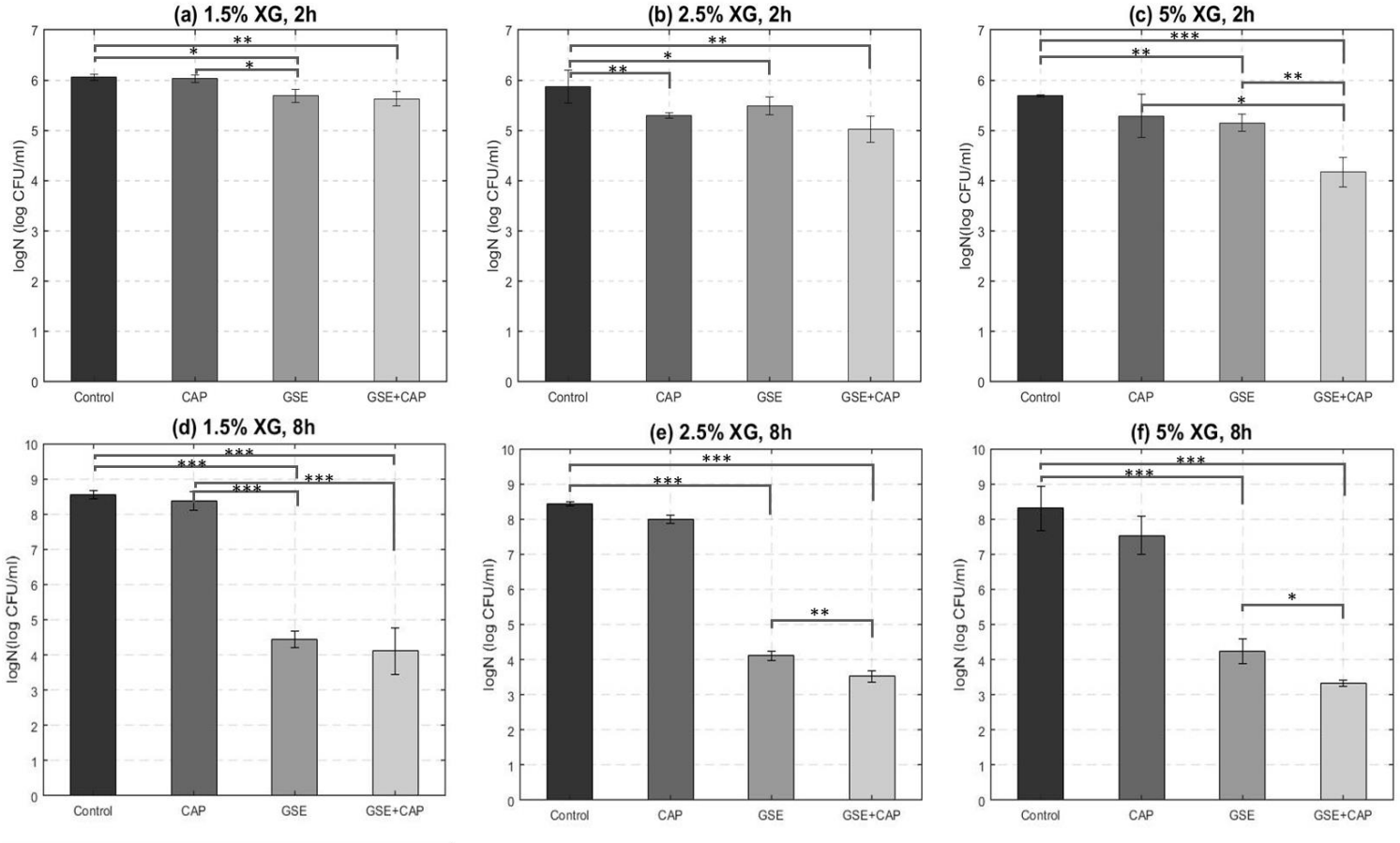
(a) 1.5% XG, 2h
(b) 2.5% XG, 2h
(c) 5% XG, 2h
(d) 1.5% XG, 8h
(e) 2.5% XG, 8h
(f) 5% XG, 8h
logN (log CFU/ml)
logN(log CFU/ml)
Control
CAP
GSE
GSE+CAP

Figure 5

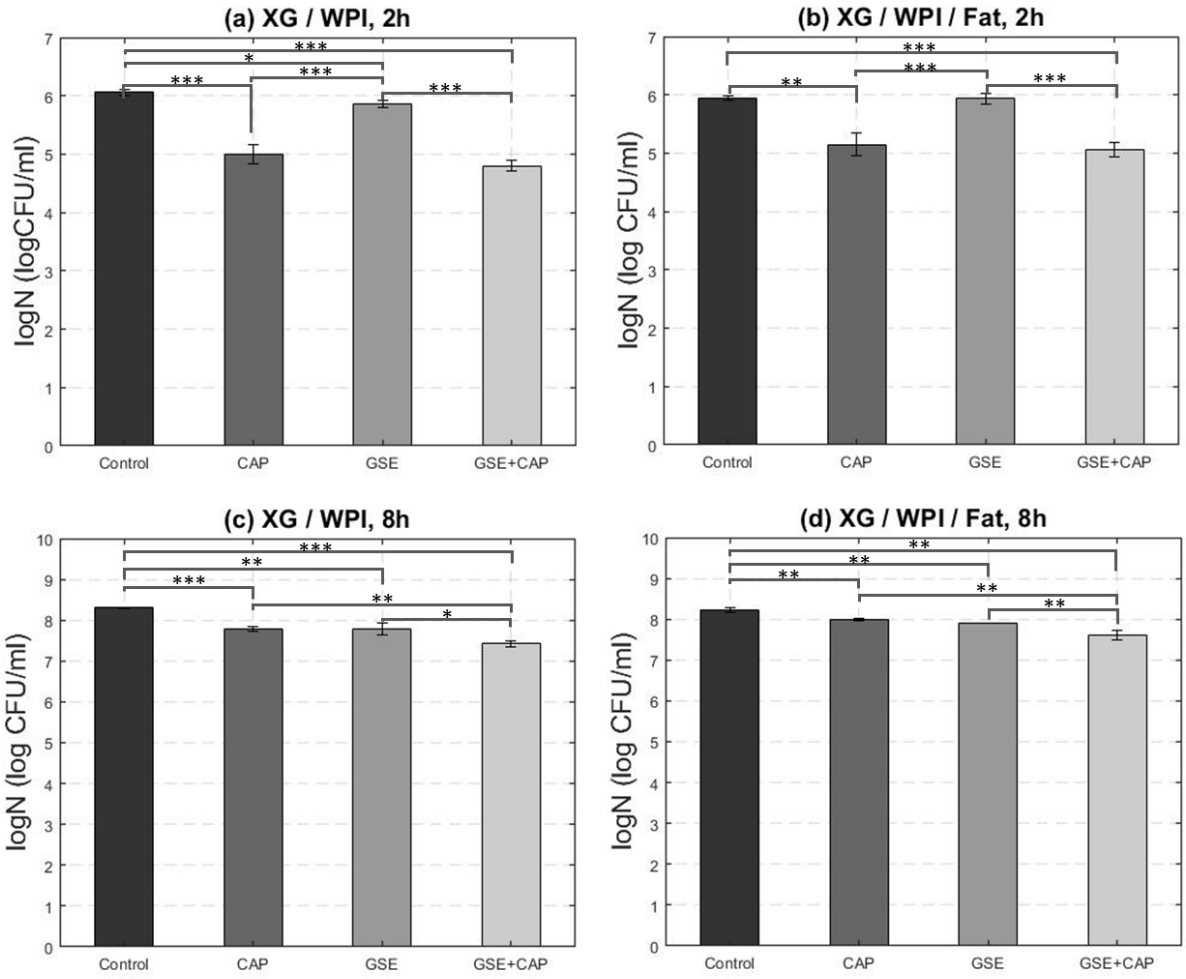
(a) XG / WPI, 2h
logN (logCFU/ml)
Control
CAP
GSE
GSE+CAP
(b) XG / WPI / Fat, 2h
logN (log CFU/ml)
(c) XG / WPI, 8h
(d) XG / WPI / Fat, 8h

Appendix

Analysis of the developed biphasic and triphasic 3D models with a rheometer confirmed their viscoelasticity, similarly to our previously reported analysis for the monophasic systems (Costello et al., 2018). The storage modulus, G′, is much larger than the loss modulus, G″, with a loss tangent tanδ < 1 for all gels, indicating that the elastic component dominates the flow properties (Figure A1 and also Table 1).

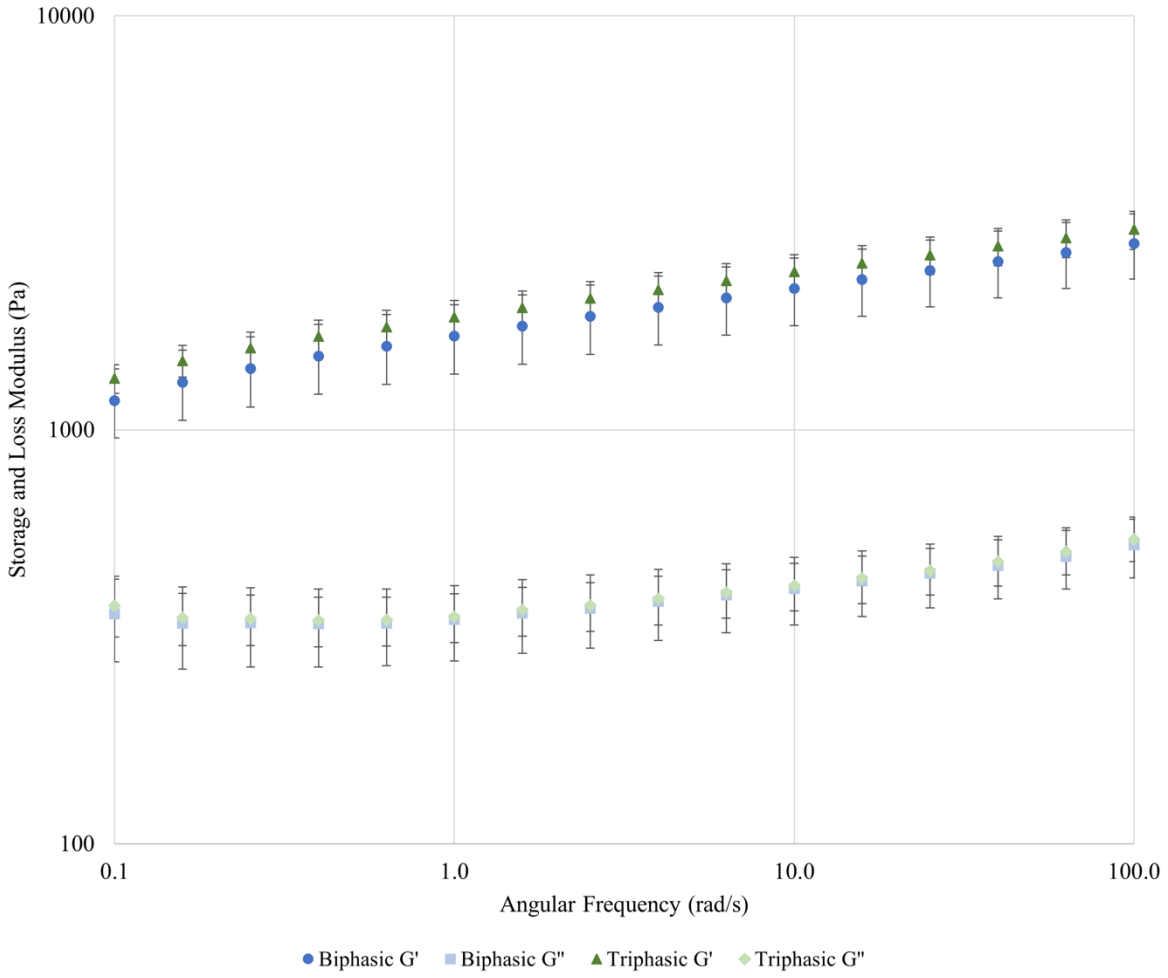

Figure A1. Rheological characterization of the biphasic and triphasic 3D viscoelastic models. Storage modulus G' and the loss modulus G'' as a function of the angular frequency at 37 °C.

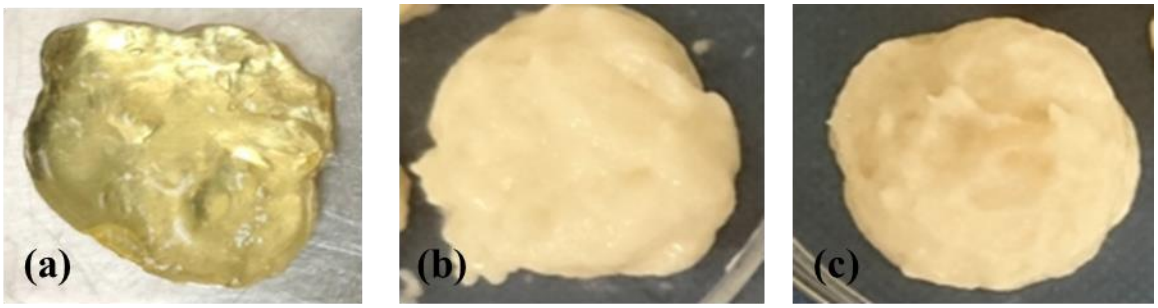

Figure A2. Images of the developed 3D models: (a) monophasic (XG), (b) biphasic (XG/ WPI), (c) triphasic (XG/ WP/ Fat) system.

Table A1. RONS produced by CAP device at different flow rates using compressed air.

Flow rate (L/min)	NO (ppm)	NO_2 (ppm)	O_3 (ppm)
0.1	764	609	
0.2	738	449	
0.3	557	350	
0.4	354	327	
0.5	227	352	
0.6	92	411	
0.7	9	300	
0.8			1.1
0.9			45
1.0			316
1.5			827
2.5			1074
3.0			1176
3.5			1170
4.0			1140
4.5			1014
5.0			959